THE ASTROPHYSICAL JOURNAL, 439:202–223, 1995 January 20

NEAR-INFRARED SPECTRA OF COMPACT STELLAR WIND SOURCES AT THE GALACTIC CENTER

S. LIBONATE,[1,2] J. L. PIPHER,[1,3] AND W. J. FORREST[1,4]
Department of Physics and Astronomy, University of Rochester, Rochester, NY 14627
AND
M. L. N. ASHBY[1,5]
Department of Astronomy, Cornell University, Ithaca, NY 14853
Received 1993 December 27; accepted 1994 July 27

ABSTRACT

We present high- and low-resolution, *H*- and *K*-band spectra of nine compact 2.2 μm Galactic center sources in which we clearly detect He I 2.058 μm emission, including the AF source, IRS 13, IRS 1W, IRS 16NE, IRS 16NW, IRS 16C, IRS 16SW, IRS 34, and IRS 6E. We have also obtained comparison spectra of both a luminous blue variable (LBV) and a WR star (P Cygni and HD 192163, respectively).

Our *H*- and *K*-band spectrum of the LBV P Cygni strongly resembles the near-infrared spectra of known WN9/Ofpe stars. Our spectra of the Galactic center sources share many characteristics in common with our spectrum of P Cygni. The spectra all show emission lines of H I and He I with large He I/H line flux ratios. Some have permitted and forbidden lines of Fe II. Brackett line widths and ratios indicate the presence of strong stellar winds. In contrast to the spectrum of the WR star, none of the Galactic center sources show evidence of He II emission lines in their spectra, suggesting that none of the Galactic center sources are WR stars.

Our high-resolution *H*-band spectrum of the AF source differs from previously published low-resolution *H*-band spectra in that it is rich in emission lines. Furthermore, we find two distinct *spectral* components to the AF source separated in space by a few arcseconds. We identify both the emission-line component of the AF source and an exciting source of IRS 13 as an LBV or WN9/Ofpe star. Our results, when combined with the results of others, also suggest that IRS 16NE, IRS 16C, IRS 16NW, IRS 34, and a component of IRS 6E are early-type, emission-line stars. The argument for IRS 16SW, however, is less compelling. We find no evidence for a compact He I emission-line source at IRS 1W. This result contradicts previous findings, suggesting that the He I source at IRS 1W may be variable. If the He I lines in IRS 1W are truly variable, a stellar component of IRS 1W may be an LBV, because LBVs are known to have variable line emission on short timescales. The nine Galactic center wind sources appear to contribute a significant fraction of the total luminosity of the central few parsecs of the Galaxy.

Subject headings: Galaxy: center — infrared: stars — stars: emission-line, Be — stars: mass loss — stars: Wolf-Rayet

1. INTRODUCTION

Far-infrared observations indicate that the Galactic center has a luminosity of approximately $10^7\ L_\odot$ (Becklin, Gatley, & Werner 1982; Davidson et al. 1992). Two sources of the luminosity have been proposed: a massive black hole (Genzel & Townes 1987), and a cluster of massive young hot stars, formed in a starburst 10^6–10^7 years ago (Rieke & Lebofsky 1982).

Dynamical evidence (Herbst et al. 1993b; Lacy, Achterman, & Serabyn 1991; Sellgren et al. 1990) indicates a mass concentration of $10^6\ M_\odot$ within a few arcseconds of the unresolved, nonthermal radio source, Sgr A*. Many authors interpret this as evidence for the existence of a massive black hole at the position of Sgr A*. However, there are no strong NIR (near-infrared) point sources within the Sgr A* positional error circle (Herbst, Beckwith, & Shure 1993a; Eckart et al. 1993). It is improbable that the source of luminosity of the central parsec would escape detection in the NIR. It is more probable that bright NIR sources like the compact components of IRS 16 are the source of luminosity. They have blue NIR colors and little or no CO absorption in their spectra (Rieke, Rieke, & Paul 1989; Allen, Hyland, & Hillier 1990), indicating they may be hot, early-type stars.

Forrest et al. (1987) discovered that several of the blue NIR sources (IRS 16NE, IRS 16C, IRS 16NW, the AF source, and IRS 29) have strong Brα emission, but no 5 or 15 GHz counterparts. They argued that these weak radio, strong Brα sources are reminiscent of stars losing mass through a dense ionized wind, such as young stellar objects, Be stars, or Wolf-Rayet (WR) stars. WR stars are known to be hydrogen deficient, so it is interesting that these unusual Brα sources have anomalously large He/H ratios (Krabbe et al. 1991). WR stars are also known to have strong mass-loss winds, and some of the Galactic center sources have Brγ line widths in excess of 350 km s^{-1} (IRS 13, IRS 16NE, IRS 16C, and the AF star), while others have Brγ line widths of 150–200 km s^{-1} (IRS 1W, IRS 12N, and IRS 6E) and/or P Cygni profiles (IRS 12N, IRS 14NE). These line widths and profiles are interpreted as evidence for

[1] Visiting Astronomer, Kitt Peak Observatory which is operated by the Association of Universities for Research in Astronomy, Inc., under contract with the National Science Foundation.
[2] Now at Rochester Institute of Technology, Center for Imaging Science, 54 Lomb Memorial Dr., Rochester, NY 14623-5604. gslpci@borg.cis.rit.edu.
[3] E-mail: jlpipher@boris.pas.rochester.edu.
[4] E-mail: forrest@dudley.pas.rochester.edu.
[5] E-mail: ashby@astrosun.tn.cornell.edu.

stellar winds. Our unpublished Brα images indicate that IRS 6E and IRS 34 are also compact Brα sources with weak 5 or 15 GHz radio counterparts, suggesting that these sources may be mass-loss objects also.

The AF source was identified as a WN9/Ofpe star by Allen et al. (1990) based on the similarity of its K-band spectrum to that of WN9/Ofpe stars in the LMC. WN9/Ofpe stars and other related objects such as luminous blue variables (LBV) and WR stars are exceedingly luminous (see Appendix). Approximately 10–100 of these objects could account for the luminosity observed in the Galactic center. Krabbe et al. identify 17 "He I (emission-line) stars" (luminous, mass-losing objects) in the central parsec, including the AF source, IRS 16NE, IRS 16C, IRS 16SW, IRS 6E, IRS 1W, and IRS 13. The fact that these objects still have hydrogen in their envelopes, coupled with a nondetection (Werner et al. 1991) of the He II (7–6, 11–8) emission-line complex at 3.092 μm in the central parsec (a line strong in WR stars) implies that these objects, if they are evolved massive stars, have not yet reached the WR phase, and are relatively cool ($T \leq 30{,}000$ K).

While the above results suggest a cluster of Be stars, LBVs, and/or WN9/Ofpe stars, more information is required to unambiguously classify these compact stellar wind sources. We have obtained NIR spectra of objects in the central parsec of the Galaxy. To classify them, we make use of information which we have compiled from published NIR spectra of emission-line stars (McGregor, Hillier, & Hyland 1988a, b; Allen, Jones, & Hyland 1985). WN9/Ofpe stars and LBVs at photometric minimum (see Appendix) are found to have strong He I line emission in their near-infrared spectra with large (≥ 0.5) F(He I 2.058 μm)/F(Brγ) ratios. The median value of the F(He I 2.058 μm)/F(Brγ) ratio is larger for the WN9/Ofpe stars than for the LBVs, but the two ranges do overlap. Permitted and forbidden lines of Fe II, lines of Mg II, and other H I lines are also found in their NIR spectra. LBVs at photometric maximum (see Appendix) as well as Be stars have H I and Fe lines, but weak or nonexistent He I 2.058 μm line emission. In all of the objects discussed by McGregor et al., the ratio of the Brγ line flux to that of higher order Brackett lines is significantly smaller than expected from case B recombination, from which they deduce that the Brγ line emission is optically thick. Such Brackett line ratios are a general property of models of line emission in mass-loss flows (Simon et al. 1983; Smith et al. 1987). The precise line ratios are dependent upon the ionization structure, mass-loss rate, and flow velocity, but for a wide range of these parameters, the models predict that the ratios of the Brα and Brγ line fluxes to those of higher order Brackett lines will be smaller than given by case B. We can use this information to help differentiate between line emission from a stellar wind source and an H II region where case B recombination applies.

In this paper, we provide spectra of the nine Galactic center sources south of IRS 7 in which we clearly detect He I 2.058 μm line emission. For three of these sources (the AF source, IRS 13, and IRS 1W) we present high ($R \sim 800$) and low ($R \sim 250$) resolution H- and K-band spectra. For the remainder (IRS 6E, IRS 34, and the compact components of IRS 16), low-resolution K-band spectra are presented. For comparison, we also present the H- and K-band spectra of a WN6 star (HD 192163) and the prototypical LBV, P Cygni.

2. OBSERVATIONS AND DATA REDUCTION

Data from two observing runs of the 2.1 m telescope at Kitt Peak National Observatory with the CRSP IR spectrometer are presented in this paper. The first and largest set of spectra was obtained on the nights of 1991 June 1–5, and the second set was obtained on the nights of 1993 July 1–6. During the first run, low-resolution spectra covering the H and K bands were obtained using a grating with dispersions of 0.00587 μm pixel^{-1} and 0.00883 μm pixel^{-1} for the H and K bands, respectively. High-resolution spectra were then obtained in the 2.08–2.19 μm region at a dispersion of about 0.00144 μm pixel^{-1}, using two slightly different grating settings. During the second run, high-resolution H-band spectra were obtained at two grating settings. The spectra from one grating setting covered the 1.566–1.672 μm region of the H band at a dispersion of 0.00174 μm pixel^{-1}, while data from the second grating setting covered the 1.650–1.750 μm region at a dispersion of 0.00168 μm pixel^{-1}.

The CRSP is a long-slit spectrometer which, during our runs, incorporated a 58 × 62 InSb array. A cosmetically superior array with fewer bad pixels was installed in the CRSP between the first and second run. For both arrays, the spectra were dispersed across the long dimension of the array, and spatial information was available along the short dimension at a platescale measured to be 1.″6 pixel^{-1}. The slit was about 80″ long, 1.″7 wide, and positioned in the east-west direction. Because the slit was only 1.″7 wide and the CRSP has no slit viewing capability, it was impossible to determine directly where the split was pointed during the observations. For this reason, IRS 7 was first "peaked up" in the slit, and then the telescope was offset south to nearby regions of interest. The position of IRS 7 was checked periodically to correct for drift. We estimate that the pointing uncertainty using this method is approximately 0.″5 based on the correspondence between the nominal slit position and spatial profiles of the Galactic center sources at the nominal and adjacent slit positions.

During the first run the slit was centered on IRS 7 and then offset south in 1″ steps, scanning nearly the entire region between 3″ south and 16″ south of IRS 7. For the second run, data were obtained at the 5S, 7S, and 13S offset positions in order to obtain spectra of IRS 1, IRS 13, and the AF source, respectively. To facilitate removal of bad pixels, integrations were taken at several east-west positions for each offset position south of IRS 7. For P Cygni and the WN6 star, a similar procedure was followed.

The frames were biased-subtracted, flat-fielded, shifted spatially (to realign the sources with one another after east-west offsetting), and then co-added. Dead, noisy, and saturated pixels were flagged and then replaced with good data from other frames during the co-addition.

Source and background apertures were both selected from a single co-added frame, and the night sky emission lines were removed by subtracting the background aperture (or a linear combination of background apertures) from the source aperture. This technique made it possible to remove contamination by diffuse background emission from gas and/or faint stars. This is especially important in the central parsec of the Galaxy where the spectra of compact objects are contaminated by emission from diffuse ionized gas and a population of faint, late-type stars (Sellgren et al. 1990). Adjacent blank regions (containing no obvious sources) were used as background apertures. For P Cygni and the WN6 star, 4″ × 1.″7 source and background apertures were selected, whereas for the Galactic center sources, 1.″7 square apertures were used. The K-band Galactic center map of Simon et al. (1990), and the Galactic center source coordinates of Tollestrup, Capps, & Becklin (1989) were used to calculate the positions of the source aper-

TABLE 1

SUMMARY OF THE OBSERVATIONS

Source	IRS 7[a] Offset (α'', δ'')	Background[b] Aperture(s) (α'')	H Band[c] ($R \simeq 250$) Itime (s)	K Band[c] ($R \simeq 250$) Itime (s)	2.08–2.19 μm[c,d] ($R \simeq 850$) Itime (s)	1.57–1.75 μm[d,e] ($R \simeq 800$) Itime (s)
P Cygni	...	4, −4	30	25	100	...
HD 192163.....	...	4, −4	80	80	...	...
AF Source	−6.9, −13	−2.8	600	300	150	450
IRS 13	−3.4, −7	12.1, −3.3	600	300	150	900
IRS 1W.....	5.0, −5	3.7, 8.8[f]	600	300	150	450
IRS 16NE	2.7, −4	13.8, −25.9	600	300	150	...
IRS 16NW	0.0, −4	16.5, −23.2	600	300	150	...
IRS 16C	1.3, −5	13.4, −23.4	600	300	150	...
IRS 16SW.....	1.2, −7	10.6, −15	600	300	150	...
IRS 34	−3.2, −4	19.7, −8.3	600	300	150	...
IRS 6E-N	−5.0, −4	21.4, −6.6	600	300	150	...

[a] Average offset of the source aperture with respect to IRS 7 (positive to N and E). The positional uncertainty is $\pm 0''.5$.
[b] Average offset of the background apertures, east of the source aperture.
[c] Integration times for data obtained 1991 June.
[d] For the Galactic center sources two grating settings were used to cover this wavelength range, each setting used this integration time.
[e] Integration times for data obtained 1993 July.
[f] The IRS 16 complex lies directly west of IRS 1W, so both IRS 1W background apertures lie to the east of IRS 1W.

tures. A summary of the observations cataloging the locations of the source and background apertures as well as the dates of the observations, integration times, and spectral resolutions can be found in Table 1.

The dispersion changes from the center of the array toward the edges, resulting in curved or bowed spectral lines as illustrated by the night sky emission lines which span the entire array. At high resolution, the shift in line position in the portion of the array occupied by the central parsec of the Galaxy is less than 0.2 pixels, but this shift can result in poor sky subtraction and make it difficult to identify low-signal-to-noise features. Thus, for the high-resolution data, Gaussian fits were made to the positions of strong, isolated OH air glow lines using IRAF's IDENTIFY routine. Then, using the FITCOORDS and TRANSFORM routines in IRAF, a least-squares fit was applied to constrain the line centers to fall as close as possible to their laboratory values in order to remove the spectral line curvature and wavelength calibrate the frames. After this fit, the residuals for the sky lines in the high-resolution spectra were typically found to be less than 2 Å. For the low-resolution data the night sky emission lines in the background apertures were used to determine the wavelength calibration.

The high-resolution wavelength calibration was checked by comparing the line centers for our high-resolution K-band spectrum of the planetary nebula NGC 7027 to the FTS spectrum of Treffers et al. (1976). Our line centers agreed with their determinations to within 30 km s^{-1}. In the general case, the uncertainty will be determined by the uncertainty in the fits to the profiles of both the OH lines used to calibrate the spectra and to the emission lines in the final spectra. Gaussians were fitted to the line profiles using IRAF's NGAUSSFIT procedure which varies the fit parameters (line center, amplitude, line width, and continuum) to minimize χ^2, and then uses the rms deviation of the data to calculate the uncertainties in the fit parameters. On average, the uncertainty in the fits to the OH airglow lines was slightly less than 3 Å. In the K-band Galactic center spectra the uncertainty in line center ranged from 1 to 3 Å, while in the H band it was 2–7 Å. The fit is best at Brγ where, assuming that the line profile is well approximated by a Gaussian, the uncertainty in our line center determination is approximately 50 km s^{-1} for the Galactic center sources. A representative example of the fit to the Brγ line (for the AF source) is shown in Figure 1.

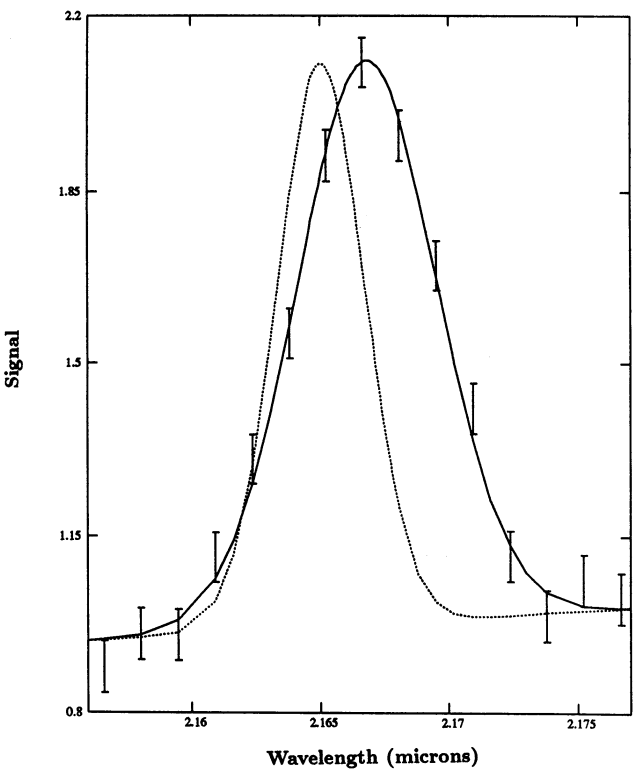

FIG. 1.—Our best fit to the Brγ line profile of the AF source (*solid line*), representative of the Galactic center spectra. The error bars denote the rms deviation of the data. A Gaussian profile assuming the line center and FWHM (convolved with our instrumental profile) for the AF source taken from Herbst et al. (1993b) is overplotted (*dotted line*) for comparison.

The measured FWHM of narrow lines in our high-resolution 2.08–2.19 μm spectra is approximately 350 km s^{-1}. The value is larger than the pixel size ($\sim$200 km s^{-1}) due to the blur of the spectrometer optics and the fact that the CRSP slit is undersampled (only 1.1 pixels over the geometrical slit). For line widths greater than 350 km s^{-1} (the minimum line width that can be clearly resolved) the uncertainty in our line-width determinations (as calculated by NGAUSSFIT) is approximately 60 km s^{-1} for the Brγ line in the Galactic center spectra.

Wavelength-calibrated spectra were divided by the spectra of standard stars to remove the telluric absorption features. For the low-resolution K-band Galactic center data, the 2.0–2.2 μm spectrum of the Galactic center M supergiant IRS 7 was spliced to the spectra of a B0V and an F7V star to create a composite standard star. In removing the telluric features from the low-resolution H-band spectra, the B0V and F7V stars were used. IRS 7 and the B0V star were used for the high-resolution K-band data. Standard star spectra of different spectral types were compared so that photospheric and telluric absorption features could be identified, and the photospheric features subsequently removed. For the H-band data taken during the second run, a K1III star was employed.

The spectra were then flux-calibrated by multiplying the ratioed spectra by a blackbody function fit to the H and K flux densities of the standard star used. The calibration was checked by comparing the continuum of the final spectrum of P Cygni to published H and K flux densities. The agreement was within 10%. We also compared our Brγ line flux to that measured by Felli et al. (1985) and again found the agreement to be within 10%. For the Galactic center sources, we found that the agreement between our low- and high-resolution line flux determinations to be approximately 15%. Furthermore, there was some uncertainty introduced by our choice of continuum. We estimate that the total uncertainty in our flux determinations is approximately 20%. We found no significant difference in the uncertainty among the different wavelength bands or spectral resolutions.

3. RESULTS

3.1. *P Cygni*

3.1.1. H *and* He I *Lines*

The low-resolution continuum of P Cygni (Fig. 2*a*) is dominated by lines of H and He I and resembles moderate resolution spectra of WN9/Ofpe stars in the LMC (McGregor et al. 1988a, b). Brackett series lines are clearly evident all the way up to Br16. The flux ratios of the higher order Brackett lines to Brγ are greater than expected from case B recombination as anticipated for wind sources. The F(He I 2.058 μm)/F(Brγ) ratio is greater than unity. The position of the Brγ line in the high-resolution spectrum (Fig. 2*b*) is consistent with no redshift, and the measured line width is 440 km s^{-1}. Line intensities identifications, and equivalent widths from the low-resolution P Cygni spectrum can be found in Table 2.

3.1.2. Mg II *Lines*

A weak feature in the low-resolution spectrum at 2.14 μm is resolved into two components in the high-resolution spectrum. We attribute this feature to the Mg II $5s\ ^2S_{1/2}$–$5p\ ^2P_{3/2}$ 2.137 μm, $5s\ ^2S_{1/2}$–$5p\ ^2P_{1/2}$ 2.144 μm doublet. This line identification has also been made in the spectra of southern-hemisphere LBVs (McGregor et al. 1988b). These lines are excited by Lyβ fluorescence (Bowen 1947). The transition from the Mg II ground state to the $5p\ ^2P_{3/2}$ level occurs at 1025.97 Å, and the transition to the $5p\ ^2P_{1/2}$ level occurs at 1026.11 Å (Simon & Cassar 1984). Both these transitions are close in wavelength to Lyβ (1025.72 Å) The differences in wavelength from Lyβ correspond to velocity shifts of 73 and 116 km s^{-1} for the $5p\ ^2P_{3/2}$ and $5p\ ^2P_{1/2}$ lines, respectively. Thus the strength of these Mg II lines will depend on the extent to which Lyβ is Doppler broadened. Because the transition from the Mg II ground state to the $5p\ ^2P_{3/2}$ level lies closer to Lyβ in wavelength, and because $5p\ ^2P_{3/2}$ has a greater statistical weight, the 2.137 μm transition should be the stronger line. The fact that the strength of the 2.144 μm component is $\sim$70% the strength of the 2.137 μm line implies that Lyβ is broad. This argues for

TABLE 2

LINE IDENTIFICATIONS, FLUXES, AND EQUIVALENT WIDTHS FOR P CYGNI

Observed Wavelength (μm)	Line Identification	Observed Flux[a] ($\times 10^{-18}$ W/cm^2)	Dereddened Flux[b] ($\times 10^{-18}$ W/cm^2)	Equivalent Width (Å)
1.589	H I 14–4 (1.588 μm)	4.8	5.4	11
	[Fe II] $a\ ^4F_{7/2}$–$a\ ^4D_{3/2}$ (1.598 μm)			
1.613	H I 13–4 (1.611 μm)	2.6	3.5	6
1.643	H I 12–4 (1.644 μm)	2.8	3.4	7
	[Fe II] $a\ ^4F_{9/2}$–$a\ ^4D_{7/2}$ (1.644 μm)			
1.684	H I 11–4 (1.680 μm)	5.4	6.9	14
	Fe II $z\ ^4F_{9/2}$–$c\ ^4F_{9/2}$ (1.688 μm)			
1.702	He I $3p\ ^3P$–$4d\ ^3D$ (1.700 μm)	4.6	6.0	12
1.738	H I 10–4 (1.736 μm)	8.6	11.7	25
	N IV 9–8 (1.736 μm)			
1.955	H I 8–4 (1.945 μm)	4.3	5.3	18
2.062	He I $2s\ ^1S$–$2p\ ^1P$ (2.058 μm)	15.3	18.1	73
2.087	Fe II $z\ ^4F_{3/2}$–$c\ ^4F_{3/2}$ (2.091 μm)	1.5	1.7	7
2.114	He I $3p\ ^3P$–$4s\ ^3S$ (2.112 μm)	2.2	2.5	11
	He I $3p\ ^1P$–$4s\ ^1S$ (2.113 μm)			
2.140	Mg II $5s\ ^2S_{1/2}$–$5p\ ^2P_{3/2}$ (2.137 μm)	3.1	3.8	16
	Mg II $5s\ ^2S_{1/2}$–$5p\ ^2P_{1/2}$ (2.144 μm)			
2.166	H I 7–4 (2.166 μm)	8.5	10.2	45

[a] We estimate that the uncertainty in our flux determinations is 20%.

[b] To obtain the dereddened fluxes, the entire spectrum was dereddened ($A_V = 1.6$, Turner 1985) assuming a $\lambda^{-1.6}$ reddening law (Cardelli et al. 1989), and the fluxes were remeasured.

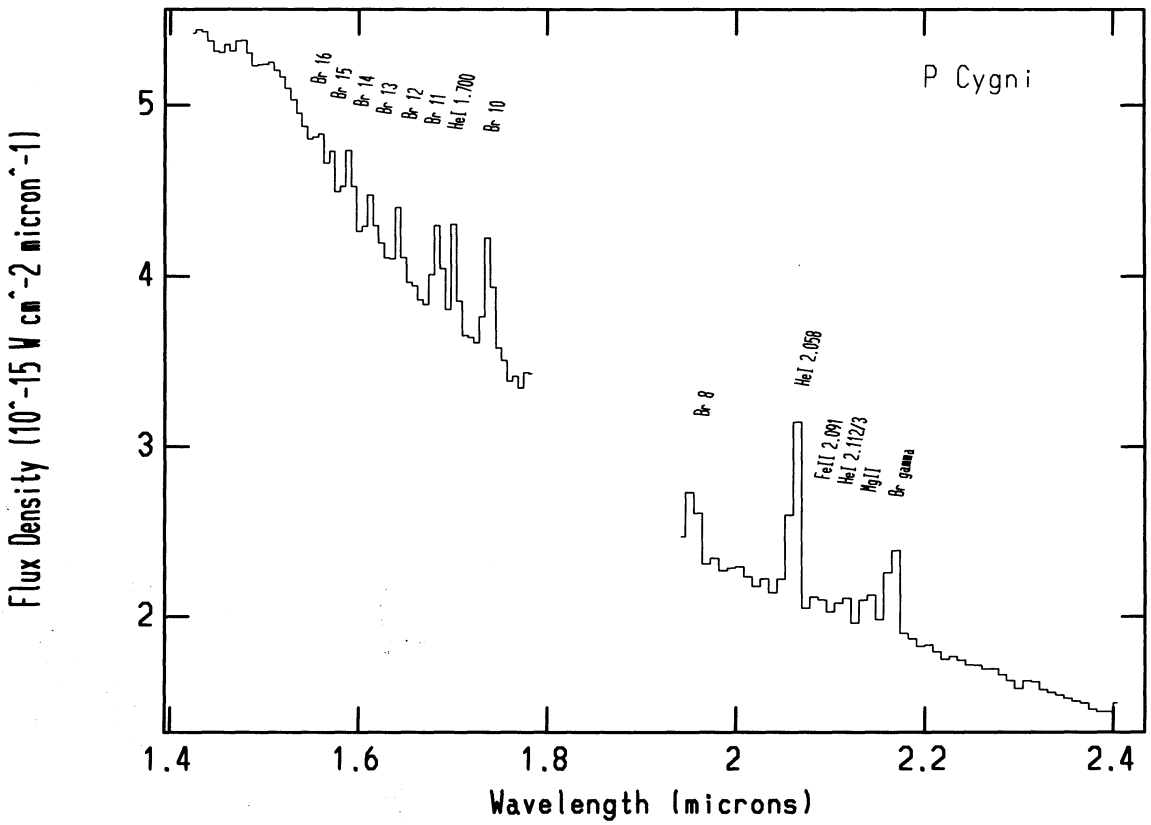

FIG. 2*a*

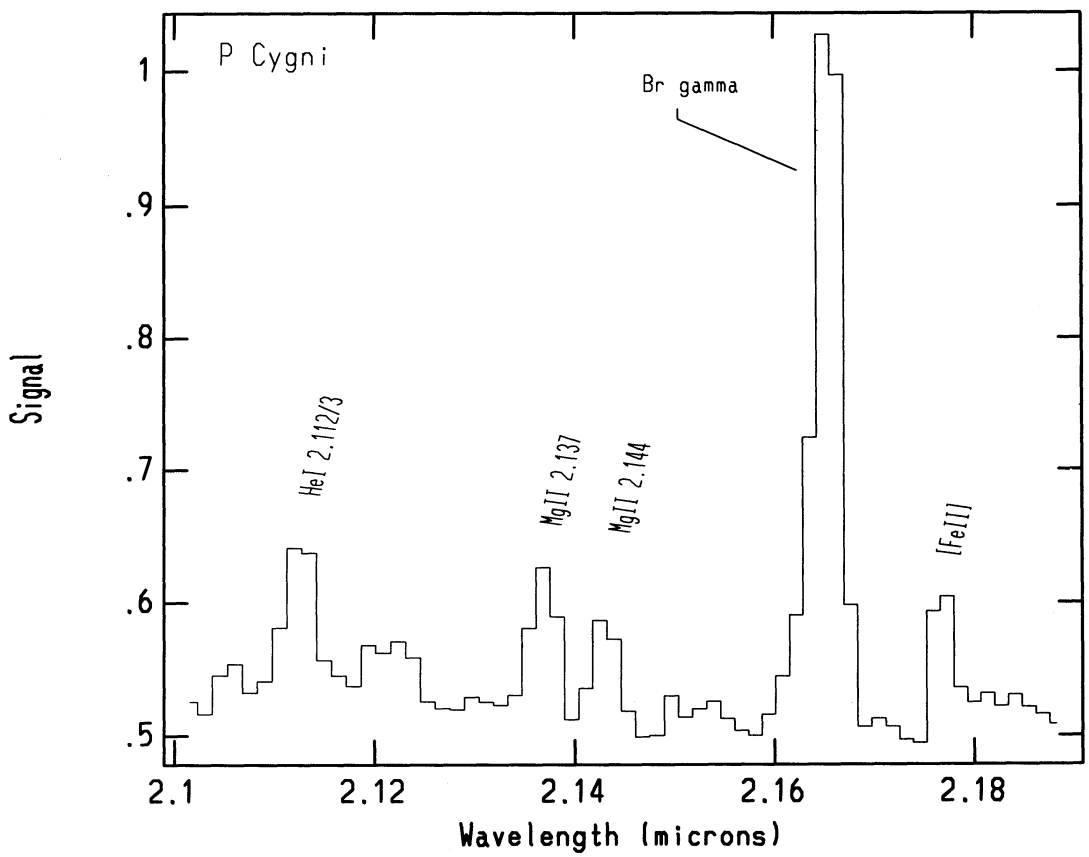

FIG. 2*b*

FIG. 2.—(*a*) *H*/*K* composite, low-resolution ($R \simeq 250$) spectrum of P Cygni. (*b*) the 2.10–2.19 μm high-resolution ($R \simeq 850$) spectrum of P Cygni. The intensity scale is arbitrary.

relatively strong stellar winds in P Cygni. The Brγ line width in our high-resolution spectrum imply stellar winds of about 200 km s^{-1}, sufficient to allow for the observed fluorescence of both Mg II lines.

3.1.3. Fe *Lines*

The only isolated Fe line evident in P Cygni's low-resolution spectrum is weak [Fe II] $z\ ^4F_{3/2}$–$c\ ^4F_{3/2}$, line emission at 2.091 μm. Stronger Fe lines are the [Fe II] $a\ ^4F_{9/2}$–$a\ ^4D_{7/2}$ transition at 1.644 μm and the Fe II $z\ ^4F_{9/2}$–$c\ ^4F_{9/2}$ line at 1.688 μm. There are emission lines at these wavelengths in our spectrum, but they are blends with Brackett lines. In the high-resolution spectrum there is also a weak feature at $\sim$2.18 μm. The shape of the line implies that it is a blend of the [Fe II] $b\ ^4F_{3/2}$–$a\ ^2F_{5/2}$ and $a\ ^4G_{9/2}$–$b\ ^2D_{9/2}$ lines at 2.179 and 2.182 μm. These lines have been observed in the spectrum of Eta Carina, another LBV (Allen et al. 1985).

3.1.4. *Unidentified Features*

There are also weak features at 2.105 μm, and 2.121 μm in the high-resolution spectrum of P Cygni. The 2.105 μm line may be due to the C III $5p\ ^1P$–$5s\ ^1S$ transition at 2.108 μm which is found in WC stars. There are two possible identifications for the 2.121 μm line: the C III $4d\ ^1D$–$4p\ ^1P$ transition at 2.122 μm found in WC stars, and the 2.121 μm H_2 1–0 $S(1)$ transition. If the latter is correct, this would be the first time H_2 emission was observed in this type of object. Since CO emission has been observed in several early-type, emission-line stars (McGregor et al. 1988b), H_2 emission is not unreasonable. The CO emission in emission-line stars must arise from a separate, circumstellar region well shielded from the hot photosphere of the exciting source. Since the objects discovered to have strong CO emission also showed dust continua, it was reasoned that the dust may help provide a cooler circumstellar environment more favorable to CO emission. Such a shielding mechanism may also exist in P Cygni, although no CO emission has been detected in the IR (Geballe & Persson 1987). Furthermore, P Cygni's 2–20 μm continuum can be fitted by a free-free model (Gehrz, Hackwell, & Jones 1974) and is not interpreted as dust shell emission. No other strong H_2 transitions occur in wavelength range we covered at high-resolution, so this possible identification of the 2.121 μm line cannot be confirmed.

3.2. *HD 192163, a WN6 Star*

The spectrum of the WN6 star, HD 192163 (Fig. 3), is dominated by recombination lines of completely ionized helium (as expected from the higher temperature of WR stars compared with LBVs) blended with contributions from He I and H I. The strongest feature by far is the He II 9–6, 14–7 blend at 1.48 μm, but other He II transitions to the $n = 7$ level are also seen. The He II 12–7, 1.692 μm line should contain unresolved contributions from Fe II at 1.688 μm, and He I at 1.700 μm. The fact that the 1.692 μm line appears broader than the other He II lines in the H bands lends credence to this assumption. Strong transitions to the $n = 8$ level of He II are also evident. Weak He II transitions to the $n = 9$ level can be seen in the long-wavelength end of the K band. Line intensities, identifications, and equivalent widths can be found in Table 3.

The He II transitions from even-numbered levels to the $n = 8$ level occur at the same wavelengths as He I ($n = 4$) transitions and the Brackett lines of hydrogen. By comparing the even and

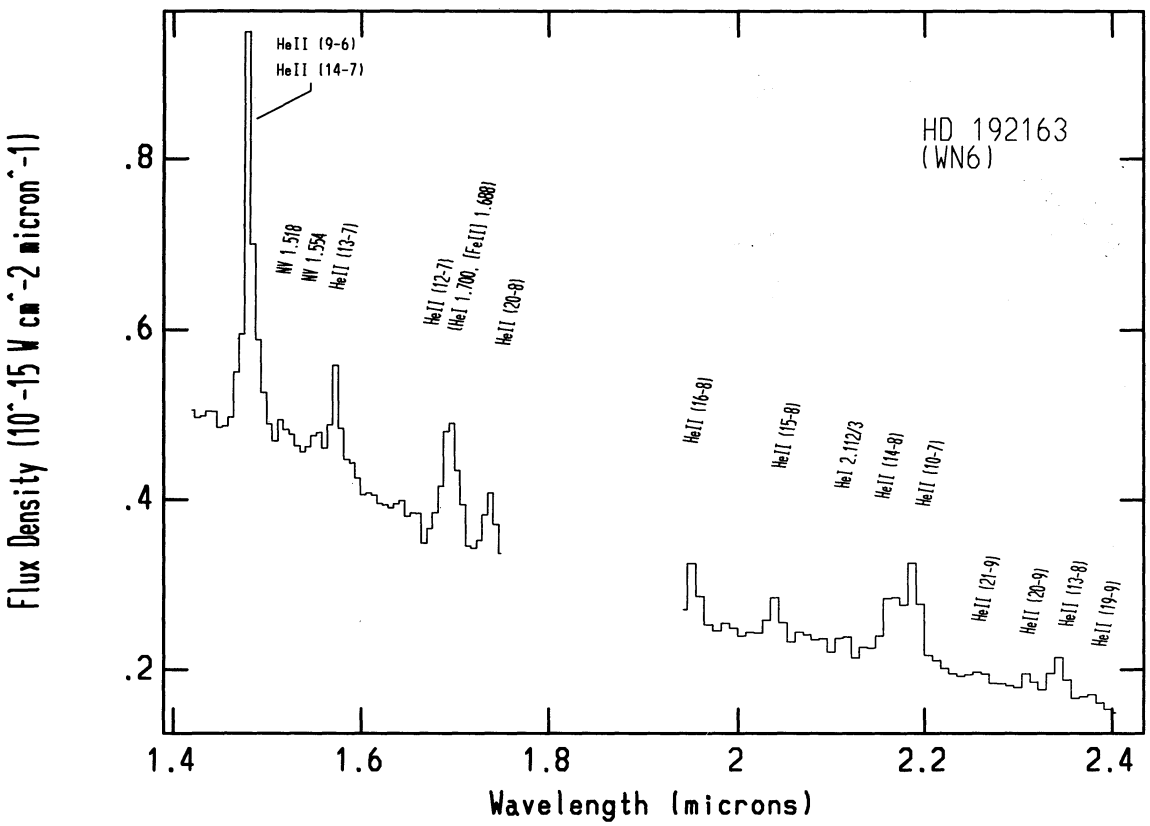

FIG. 3.—H/K composite, low-resolution ($R \simeq 250$) spectrum of the WN6 star HD 192163

TABLE 3

LINE IDENTIFICATIONS, FLUXES, AND EQUIVALENT WIDTHS FOR HD 192163

Observed Wavelength (μm)	Line Identification	Observed Flux[a] ($\times 10^{-18}$ W/cm^2)	Equivalent Width (Å)
1.479	He II 9–6 (1.477 μm)	4.8	95
	He II 14–7 (1.489 μm)		
1.517	N V $^3P\ ^2P$–$3d\ ^2D$ (1.518 μm)	0.4	9
1.553	N V 10–9 (1.554 μm)	0.4	8
1.572	He II 13–7 (1.572 μm)	1.2	28
	He II 15–4 (1.570 μm)		
	He II 30–8 (1.570 μm)		
1.694	He II 12–7 (1.692 μm)	3.0	80
	He I $3p\ ^3P$–$4d\ ^3D$ (1.700 μm)		
	Fe II $z\ ^4F_{9/2}$–$c\ ^4F_{9/2}$ (1.688 μm)		
1.736	He II 20–8 (1.736 μm)	1.1	33
	H I 10–4 (1.736 μm)		
	He I 10–4		
	N IV 9–8 (1.736 μm)		
1.953	H I 16–8 (1.945 μm)	1.0	35
	H I 8–4 (1.945 μm)		
2.038	He II 15–8 (2.038 μm)	0.8	30
2.113	He I $3p\ ^3P$–$4s\ ^3S$ (2.112 μm)	0.3	14
	He I $3p\ ^1P$–$4s\ ^1S$ (2.113 μm)		
2.165	He II 14–8 (2.166 μm)	1.7	85
	H I 7–4 (2.166 μm)		
	He I 7–4		
2.188	He II 10–7 (2.189 μm)	2.0	100
2.259	He II 21–9 (2.260 μm)	0.2	9
2.311	He II 20–9 (2.314 μm)	0.3	18
2.343	He II 13–8 (2.347 μm)	1.0	56
2.377	He II 19–9 (2.379 μm)	0.3	17

[a] We estimate that the uncertainty in our flux determinations is 20%.

odd He II transitions to $n = 8$, the He I and H I contributions can be estimated. We conclude that about half of the emission in the 2.166 μm line [He II 14–8, He I (7–4), Brγ] is due to He I and H I. This result can then be used to estimate the H I, He I, and He II contributions at 1.736 μm, which leads to the conclusion that there is a contribution made by N IV 9–8 to the 1.736 μm line. Since this is a WN star we expect to see nitrogen lines in the spectrum and further identify lines at 1.517 and 1.553 μm as N V $3p\ ^2P$–$3d\ ^2D$ and N V 10–9, respectively.

3.3. *The AF Source*

3.3.1. *Low-Resolution K-Band Spectrum*

As demonstrated by Allen et al. (1990), the low-resolution K-band spectrum of the AF source (Fig. 4*a*) is dominated by three prominent emission lines. The strongest feature is due to the 2.058 μm He I line (He I $2s\ ^1S$–$2p\ ^1P$) whose flux (Table 4) is double that of Brγ. Recall that an anomalous He I 2.058/Brγ flux ratio is observed in our spectrum of P Cygni. There is also emission from the He I 2.112/3 feature (He I $3p\ ^3P$–$4s\ ^3S$, He I $3p\ ^1P$–$4s\ ^1S$) in the spectrum of the AF source. Longward of the Brγ line there are no obvious emission lines, nor is strong CO absorption apparent at 2.3 μm and beyond.

3.3.2. 2.08–2.19 μm *High-Resolution Spectrum*

The high-resolution, 2.08–2.19 μm spectrum (Fig. 4*b*) shows the He I 2.112/3 μm feature and the Brγ line detected at low resolution (Fig. 4*a*). The He I 2.112/3 feature is redshifted by approximately 370 km s^{-1} in our spectrum, and the Brγ line is redshifted by 180 km s^{-1}. This latter value agrees with the redshifts measured by Allen et al. (1990) and at 111 km s^{-1} resolution by Najarro et al. (1993), but is in disagreement with the Fabry-Perot observations of Herbst et al. (1993b) who find a blueshift for the AF source of $\sim$70 km s^{-1}. The data of Herbst et al. (1993b) were obtained at a higher resolution than ours, but we note that for every source observed in common, our measured redshift is larger. The Herbst et al. (1993b) Brγ line profile (scaled and convolved with our instrumental profile) is overplotted with our data and line profile for comparison in Figure 1. Note that our data are not well fitted by the Herbst et al. (1993b) profile. The data are well fitted by our profile, and since OH airglow lines (observed along with the data) were used for the wavelength calibration, we have confidence in our result.

The widths of the strong lines in the high-resolution spectrum are both much broader than our instrumental profile of 350 km s^{-1}. The observed width (FWHM) of the Brγ line is 890 km s^{-1}. A deconvolution of the data and our instrumental profile results in a FWHM of approximately 800 km s^{-1}, implying very strong mass-loss winds. This is in fair agreement with the Brγ width of 700 km s^{-1} measured by Najarro et al. (1993), but disagrees with that of Herbst et al. (1993b) who measures a FWHM of 430 km s^{-1} (see Fig. 1). The observed width of the He I 2.112/3 μm feature in our spectrum (620 km s^{-1}) is narrower than that of Brγ. P Cygni absorption in the He I line will decrease its apparent width, and effectively redshift the He I line with respect to the Brγ line. Alternatively, the Brγ line may be broadened by a contribution from the He I (7–4) complex. Najarro et al. (1993) also find that the Brγ line is broader than and blueshifted with respect to the He I lines in their AF spectrum. They attribute both the line width and blueshift to a contribution from He I (7–4) transitions.

3.3.3. *Low-Resolution H-Band Spectrum*

The decrease in the AF source continuum level toward shorter wavelengths (Fig. 4*a*) results from the heavy extinction

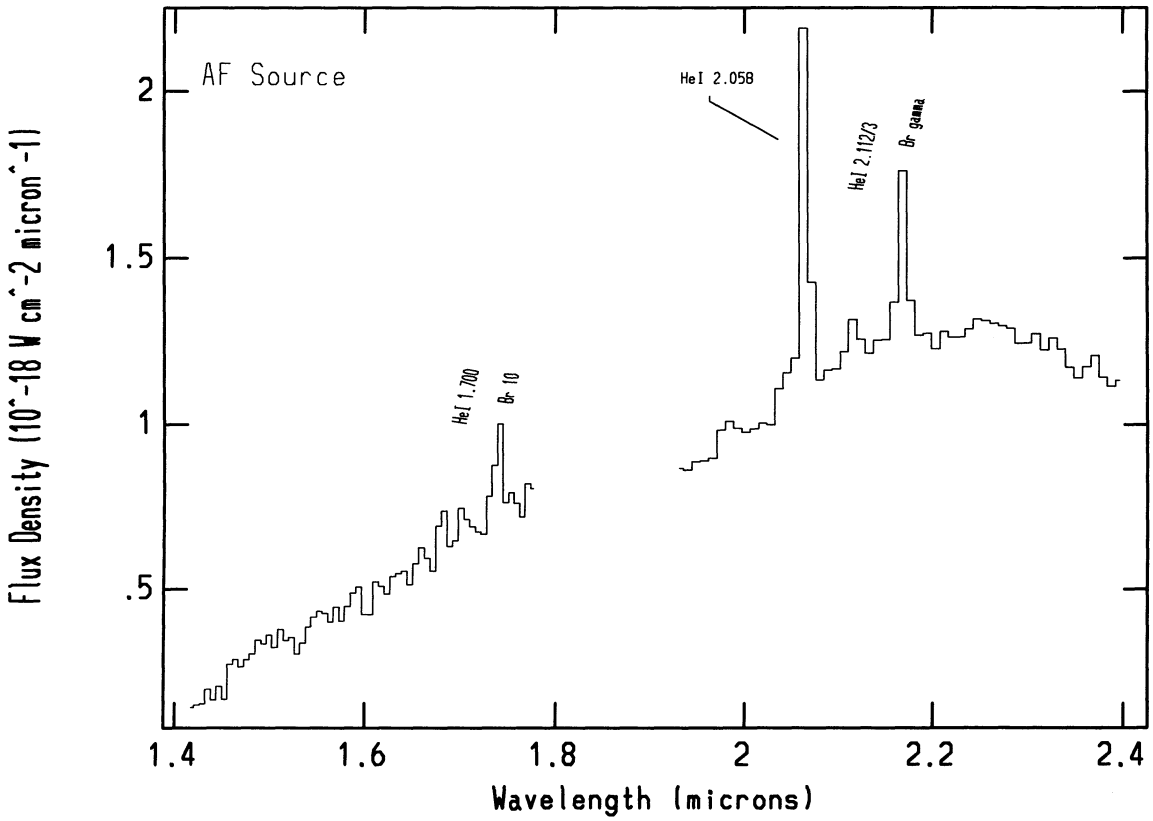

FIG. 4*a*

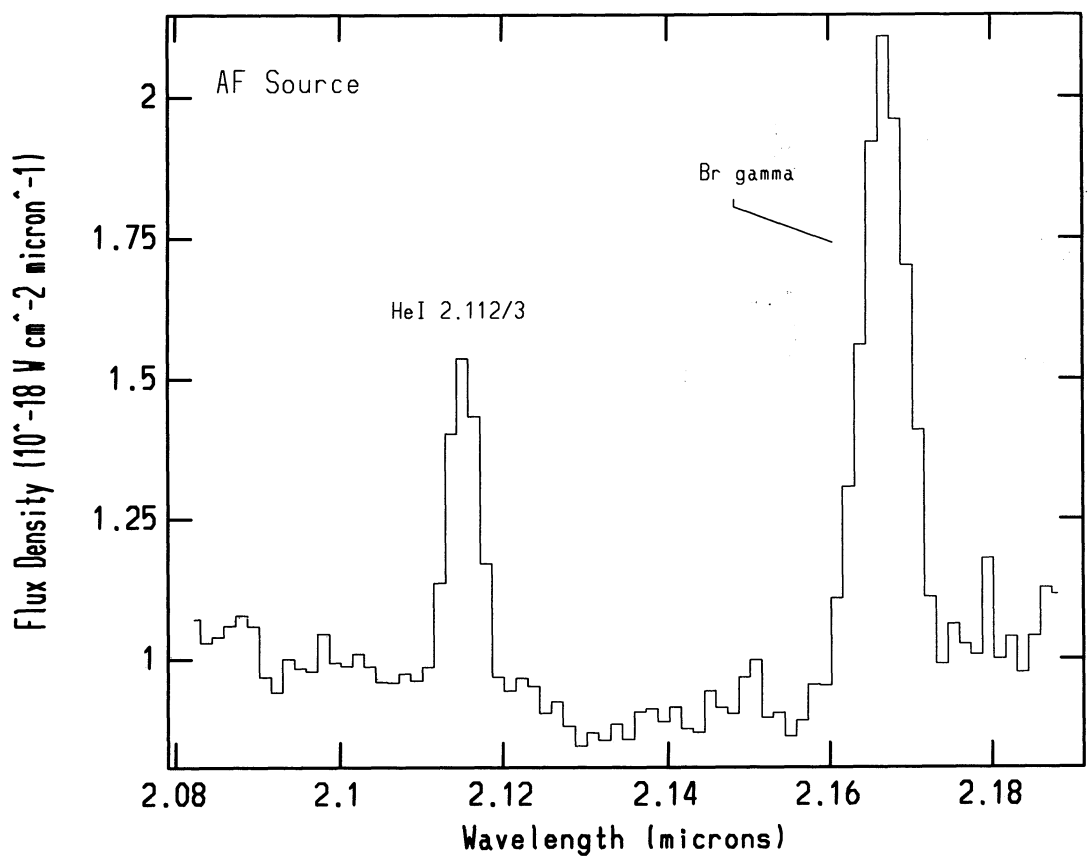

FIG. 4*b*

FIG. 4.—(*a*) *H*/*K* composite, low-resolution ($R \simeq 250$) spectrum of the AF source extracted 3″.5 west of IRS 12N with the slit was nominally positioned 13″ south of IRS 7. (*b*) High-resolution ($R \simeq 850$) *K*-band spectrum of the AF source extracted 3″.5 west of IRS 12N with the slit was nominally positioned 13″ south of IRS 7. (*c*) High-resolution ($R \simeq 800$) *H*-band spectrum of the AF source extracted 3″.5 west of IRS 12N with the slit was nominally positioned 13″ south of IRS 7.

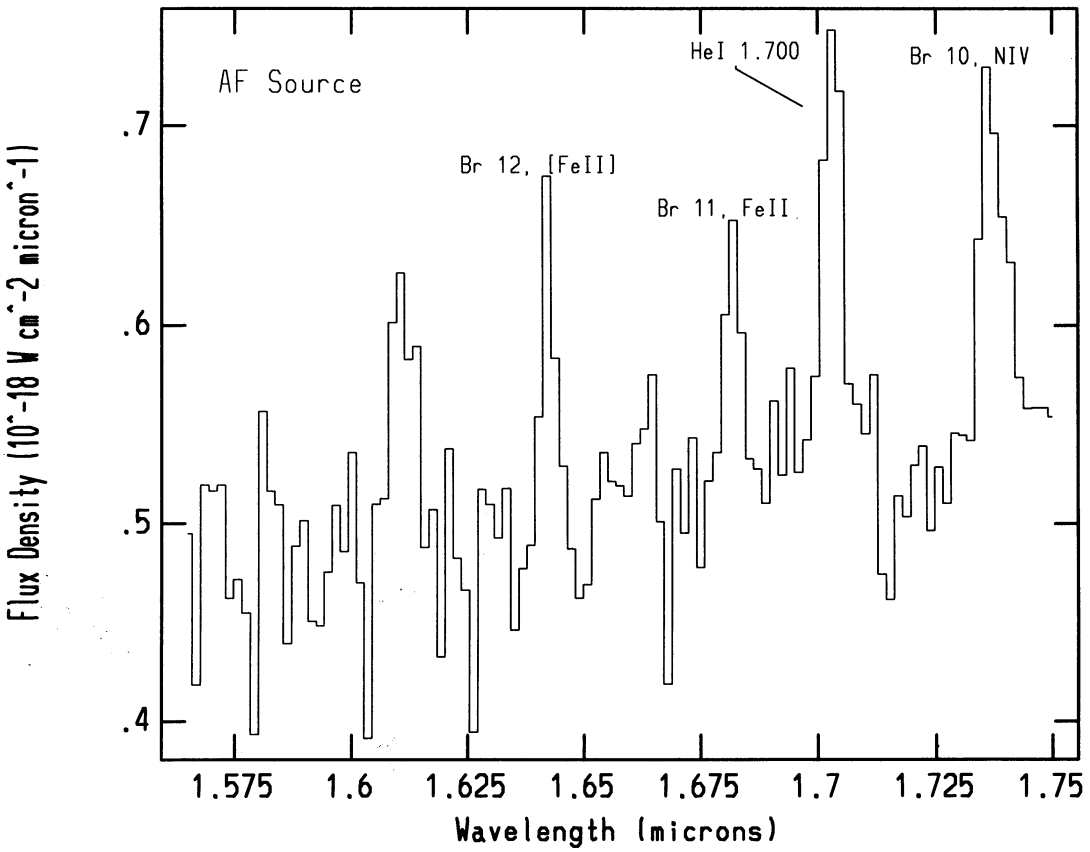

FIG. 4c

($A_V \simeq 27$ mag, Wade et al. 1987) to the Galactic center. The night sky lines are more than an order of magnitude more intense than the H-band spectrum of the AF source. As a consequence, imperfect background subtraction results in a noisy spectrum, making line identification difficult.

A convincing case for the line identifications in the *H* band can be made when the low-resolution AF spectrum is compared to a spectrum of P Cygni reddened to the extinction of the Galactic center. P. Cygni's spectrum was first dereddened ($A_V = 1.6$ mag; Turner 1985) and then reddened assuming $A_V \simeq 27$ mag (Wade et al. 1987) and a $\lambda^{-1.6}$ extinction law (Cardelli, Clayton, & Mathis 1989). This extinction law is con-

TABLE 4

LINE IDENTIFICATIONS, FLUXES, AND EQUIVALENT WIDTHS FOR THE AF SOURCE

Observed[a] Wavelength (μm)	Line Identification	Observed Flux[b] ($\times 10^{-21}$ W/cm^2)	Dereddened Flux[c] ($\times 10^{-20}$ W/cm^2)	Equivalent Width (Å)
1.6421 (10).....	H I 12–4 (1.6407 μm) [Fe II] $a\ ^4F_{9/2}$–$a\ ^4D_{7/2}$ (1.644 μm) He I (12–4)	0.6	5.7	12
1.6818 (11).....	H I 11–4 (1.6806 μm) Fe II $z\ ^4F_{9/2}$–$c\ ^4F_{9/2}$ (1.688 μm) He I (11–4)	0.7	4.6	12
1.7030 (9)	He I $3p\ ^3P$–$4d\ ^3D$ (1.7002 μm)	1.3	8.8	24
1.7372 (10).....	H I 10–4 (1.7362 μm) N IV 9–8 (1.736 μm) He I (10–4)	1.3	7.9	23
2.065[d]	He I $2s\ ^1S$–$2p\ ^1P$ (2.058 μm)	12.3	28.2	110
2.1153 (7)	He I $3p\ ^3P$–$4s\ ^3S$ (2.112 μm) He I $3p\ ^1P$–$4s\ ^1S$ (2.113 μm)	2.9	5.9	30
2.1668 (7)	H I 7–4 (2.1655 μm) He I (7–4)	7.9	14.4	82

[a] The number in parentheses is the uncertainty in Å.

[b] ±20%.

[c] To obtain the dereddened fluxes, the entire spectrum was dereddened ($A_V = 27$, Wade et al. 1987) assuming a $\lambda^{-1.6}$ reddening law (Cardelli et al. 1989), and the fluxes were remeasured.

[d] The He I $2s\ ^1S$–$2p\ ^1P$ (2.058 μm) data are from the low-resolution spectrum.

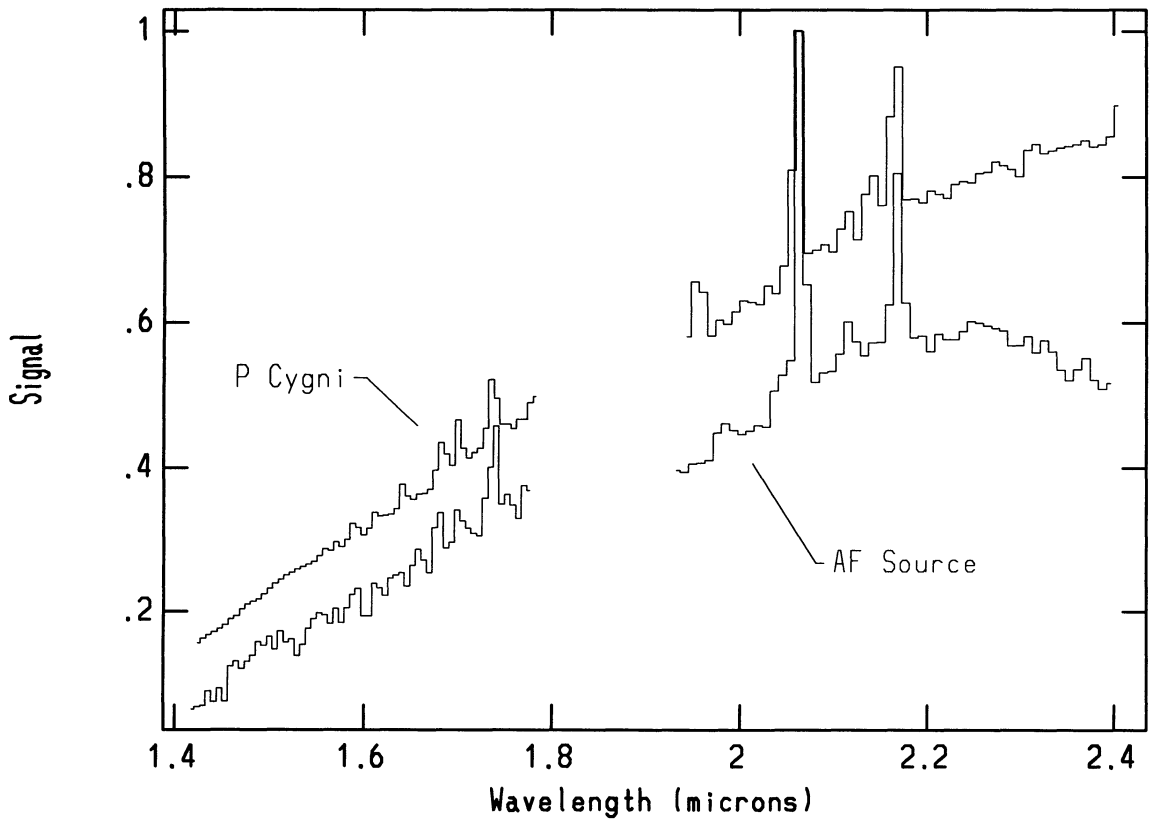

FIG. 5.—*H*/*K* composite spectrum of P Cygni from Fig. 1*a*, reddened to the extinction of the Galactic center, and then overplotted with the AF spectrum from Fig. 3*a*. The intensity scale is arbitrary. Each spectrum was normalized by the peak signal level in its 2.058 μm line.

sistent with that of Rieke & Lebofsky (1985) from observations of Galactic center sources, and is used throughout this paper. In Figure 5, the AF spectrum and the reddened P Cygni spectrum are overplotted. The two spectra appear quite similar. Features in the AF *H*-band spectrum appear to correspond to the Br15–Br10 lines and with the He I 1.700 μm line in P Cygni's spectrum, although many of these features are comparable in strength to the noise.

3.3.4. 1.57–1.75 μm *High-Resolution Spectrum*

The high-resolution 1.57–1.75 μm spectrum of the AF source (Fig. 4*c*) confirms the tentative identifications made at low resolution. We identify the lines at 1.7372, 1.7030, 1.6818, and 1.6421 μm as Br10, He I 1.700 μm, Br11, and Br12. The Br10 and Br11 lines are redshifted by approximately 200 km s^{-1}. This is in agreement with the redshift obtained from the Brγ line in our high-resolution *K*-band spectrum. As was true for the He I line in the *K* band, the He I 1.700 μm line has a larger redshift than the Brackett lines, so there is either a He I contribution to the *H*-band Brackett lines, or weak P Cygni absorption in the He I lines produces an effective redshift. The Br12 redshift ($\sim$255 km s^{-1}) is also larger than that found for Br10 and Br11, as would be the case if there were a significant contribution from the [Fe II] 1.644 μm line. The fact that the flux of the Br12 line is greater than that of the Br11 line is consistent with such a contribution from [Fe II] 1.644 μm line emission.

There is also an unidentified, apparently double-peaked feature with components 1.609 and 1.613 μm. Possible identifications are the [Fe II] line at 1.598 μm ($a\ ^4F_{7/2}$–$a\ ^4D_{3/2}$), and Br13 at 1.6109 μm, respectively. However, identifying the 1.609 μm feature as [Fe II] would imply an unacceptably large redshift. Furthermore, the strengths of the observed features are larger than one would expect for [Fe II] 1.598 μm and Br13 given the strengths of the 1.64 μm (Br12 and [Fe II]) and 1.68 μm (Br11 and Fe II) lines.

Allen et al. (1990) only identify the [Fe II] 1.644 μm line in their *H*-band spectrum, whereas we have found the *H* band of the AF spectrum to be rich in emission lines. We find this discrepancy puzzling. The original speculation that the AF source is a WN9/Ofpe star was based on the line widths and He/H ratios in its *K*-band spectrum only. Our detections of He I and Brackett lines in the *H* band provide additional information with which to identify the AF source.

Line intensities, identifications, and the equivalent widths of the AF emission features can be found in Table 4. High-resolution data were used for the flux and line center determinations for all lines except for the He I 2.058 μm line which was outside of our high-resolution band.

3.4. *IRS 13*

3.4.1. *Low-Resolution K-Band Spectrum*

The low-resolution *H*/*K*-band spectrum of IRS 13 (Fig. 6*a*) shows strong Brγ and He I 2.058 μm emission with a weak feature near 2.112 μm which is probably He I 2.112/3. The He I 2.058 μm Brγ line flux ratio is nearly unity. Overall, the IRS 13 spectrum bears a strong resemblance to the low-resolution *K*-band spectra of P Cygni (an LBV) and the AF source obtained with the same instrument (Figs. 1*a* and 3*a*).

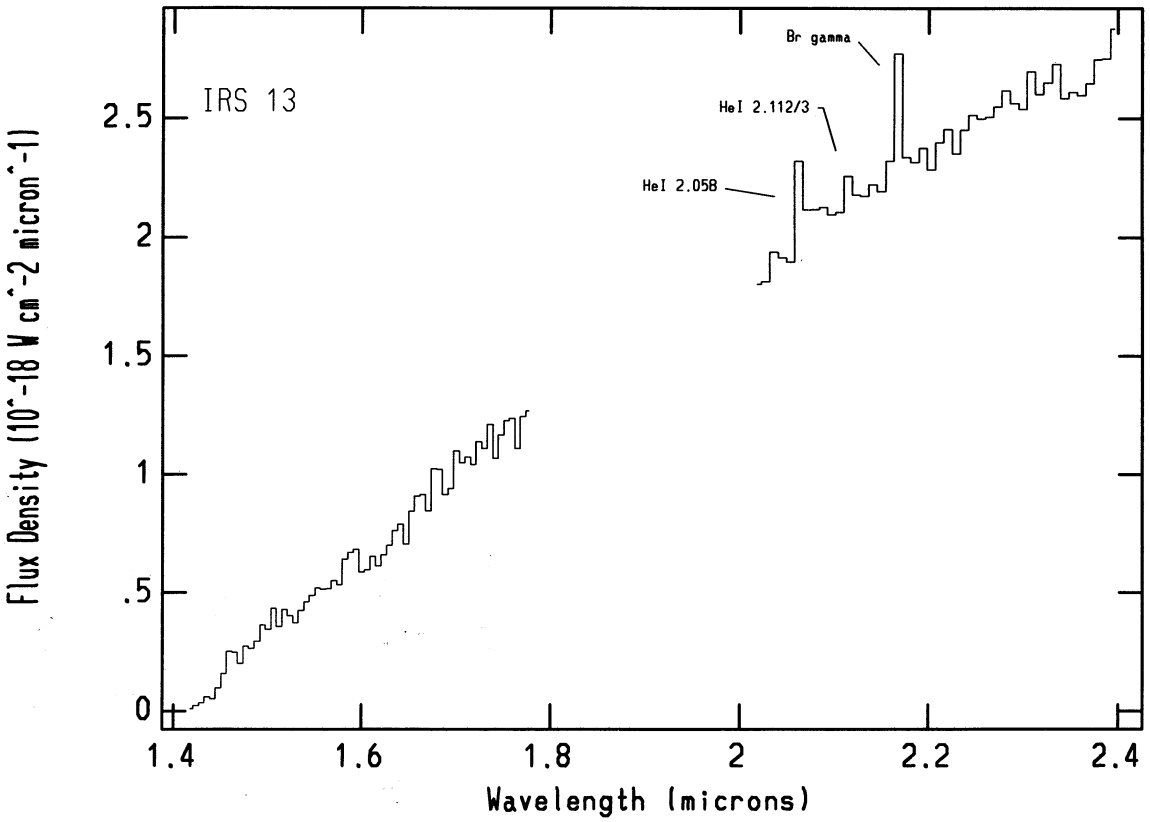

FIG. 6a

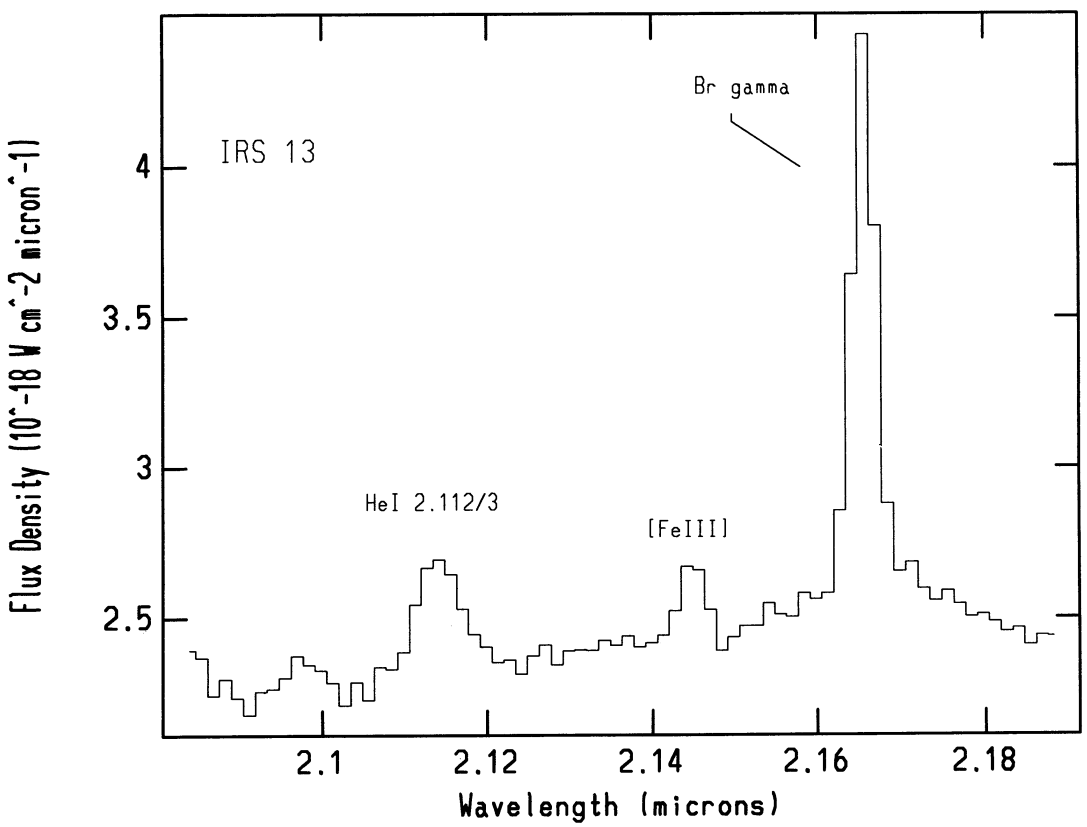

FIG. 6b

FIG. 6.—*H*/*K* composite, low-resolution ($R \simeq 250$) spectrum of Galactic center source IRS 13. (*b*) The 2.08–2.19 μm high-resolution ($R \simeq 850$) spectrum of Galactic center source IRS 13. (*c*) The 1.57–1.75 μm high-resolution ($R \simeq 800$) spectrum of Galactic center source IRS 13.

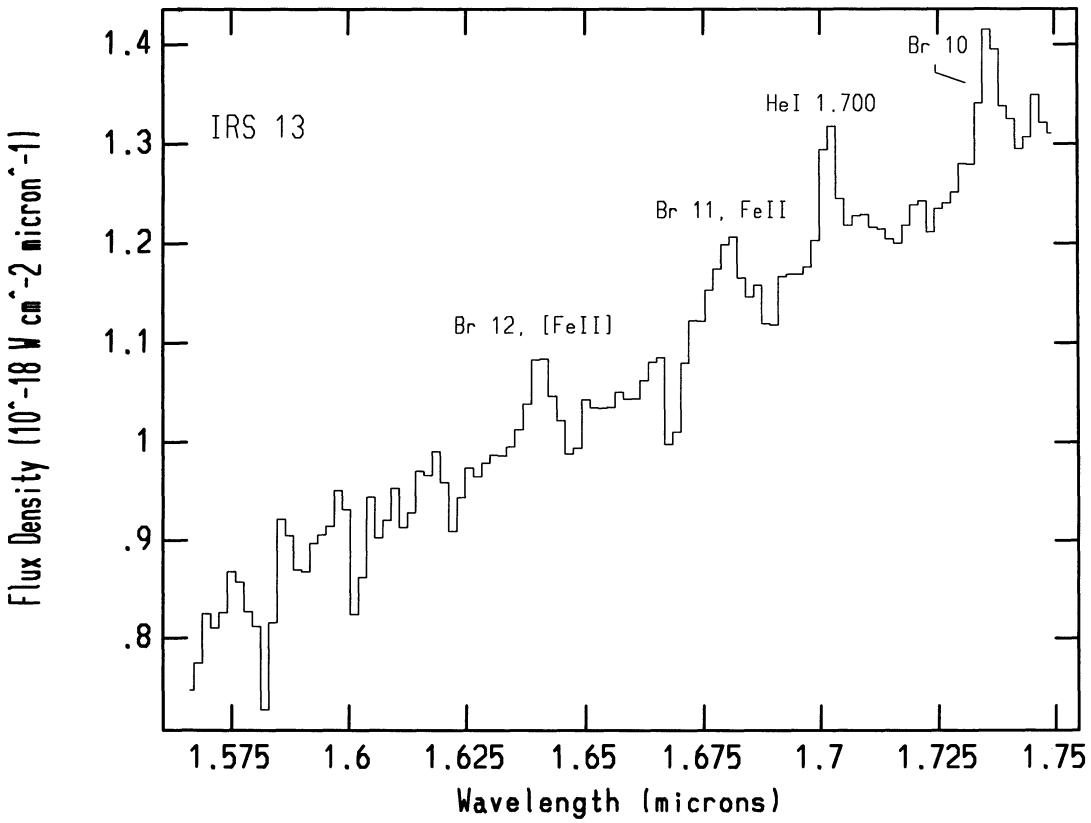

FIG. 6*c*

3.4.2. 2.09–2.19 μm *High-Resolution Spectrum*

The measured width of the Brγ line in the 2.09–2.19 μm, high-resolution spectrum of IRS 13 (Fig. 6*b*) is about 505 km s^{-1} FWHM (recall that the instrumental profile is 350 km s^{-1} FWHM). We find a blueshift of 40 km s^{-1} for the Brγ line. The weak feature observed at 2.1149 μm corresponds to the He I 2.112/3 feature. The He I line appears redshifted relative to the Brγ line, as we observed in the AF source.

There is also a weak feature at 2.1449 μm in our high-resolution spectrum. We consider several possible identifications. The Mg II $5s\ ^2S_{1/2}$–$5p\ ^2P_{3/2}$ (2.137 μm), $5s\ ^2S_{1/2}$–$5p\ ^2P_{1/2}$ (2.144 μm) doublet observed in P Cygni is one possibility, but we discount the 2.137 μm component should be the stronger

TABLE 5

LINE IDENTIFICATIONS, FLUXES, AND EQUIVALENT WIDTHS FOR IRS 13

Observed[a] Wavelength (μm)	Line Identification	Observed Flux[b] ($\times 10^{-22}$ W/cm^2)	Dereddened Flux[c] ($\times 10^{-20}$ W/cm^2)	Equivalent Width (Å)
1.6402 (10).....	H I 12–4 (1.6407 μm) [Fe II] $a\ ^4F_{9/2}$–$a\ ^4D_{7/2}$ (1.644 μm) He I (12–4)	5.3	4.5	5
1.6798 (11).....	H I 11–4 (1.6806 μm) Fe II $z\ ^4F_{9/2}$–$c\ ^4F_{9/2}$ (1.688 μm) He I (11–4)	7.2	5.2	6
1.7019 (9).....	He I $3p\ ^3P$–$4d\ ^3D$ (1.7002 μm)	6.9	4.8	6
1.7362 (9).....	H I 10–4 (1.7362 μm) He I (10–4)	7.4	5.0	6
2.065[d].....	He I $2s\ ^1S$–$2p\ ^1P$ (2.058 μm)	44	10.1	23
2.1149 (7).....	He I $3p\ ^3P$–$4s\ ^3S$ (2.112 μm) He I $3p\ ^1P$–$4s\ ^1S$ (2.113 μm)	21.3	4.5	9
2.1449 (8).....	[Fe III] $^3G_3$–$^3H_4$ (2.145 μm)	12.5	1.9	6
2.1652 (7).....	H I 7–4 (2.1655 μm) He I (7–4)	72.4	12.5	28

[a] The number in parentheses is the uncertainty in Å.

[b] $\pm 20\%$.

[c] To obtain the dereddened fluxes, the entire spectrum was dereddened ($A_V = 27$, Wade et al. 1987) assuming a $\lambda^{-1.6}$ reddening law (Cardelli et al. 1989), and the fluxes were remeasured.

[d] The He I $2s\ ^1S$–$2p\ ^1P$ (2.058 μm) data are from the low-resolution spectrum.

line, and since none of the other lines in the spectrum are highly redshifted, it is unlikely that the feature at 2.1449 μm is the redshifted 2.137 μm line. Another possible identification is He I. The ratio of He I 2.112/3 μm to He I 2.146 μm in Eta Carina is similar to that observed between the 2.1147 and 2.1449 μm lines in IRS 13 (Table 5). However, the most likely identification for the 2.1449 μm line is [Fe III] $^3G_3$–$^3H_4$ at 2.1451 μm. IRS 13 happens to lie on the western rim of the bubble surrounding the Galactic center "mini-cavity" (Yusef-Zadeh, Morris, & Eckers 1989) which is a strong source of shock-excited [Fe III] line emission (Werner et al. 1992; Lutz, Krabbe, & Genzel 1993). In the Fabry-Perot images of Lutz et al., the maximum of the [Fe III] emission is coincident with the maximum of the extended Brγ line emission at IRS 13.

3.4.3. *Low-Resolution H-Band Spectrum*

In the low-resolution H-band spectrum (Fig. 6*a*) there are weak features at the positions of Brackett lines 10–13, and at the position of a He I line (1.700 μm), but there are also features which correspond to no known lines. Therefore, it is impossible to tell with certainty which features are real and which are the result of poor sky subtraction. For the AF source, a convincing case was made for the existence of low signal-to-noise lines in the low-resolution H-band spectrum by comparing its spectrum to a spectrum of P Cygni that had been reddened to the extinction of the Galactic center. Such a comparison in the case of IRS 13 proved inconclusive.

3.4.4. 1.57–1.75 μm *High-Resolution Spectrum*

Lines at 1.7362, 1.6798, and 1.6402 μm are immediately apparent in the high-resolution, 1.57–1.75 μm spectrum of IRS 13 (Fig. 6*c*) and correspond to Brackett 10–12. The Brγ/Br10 ratio is smaller than expected from case B recombination. The 1.6402 and 1.6798 μm line strengths (Table 5) are comparable to that of Br10, and the 1.6798 and 1.6402 μm line widths are broader than Br10, suggesting that these two features are blends of Br11 and Br12 with Fe lines at 1.644 μm ([Fe II] $a\ ^4F_{9/2}$–$a\ ^4D_{7/2}$), and at 1.688 μm (Fe II $z\ ^4F_{9/2}$–$c\ ^4F_{9/2}$). However, the measured feature wavelengths (1.6402 and 1.6798 μm) are blueshifted. Thus, any redshift to the features from the Fe II contribution must be offset by a blueshift from a He I contribution, unless the Fe II lines are blueshifted themselves. In 4".8, 150 km s^{-1} [Fe II] observations of the Galactic center, DePoy (1992) has found the [Fe II] 1.644 μm emission in the vicinity of IRS 13 to be blueshifted by 70–310 km s^{-1}, making the Fe contribution plausible.

Most significant of all (in terms of identifying IRS 13 as an LBV or WN9/Ofpe) is the detection of the He I 1.700 μm line whose strength is comparable to that of Br10. Unlike the Brackett lines, but like the He I 2.112/3 μm feature in the K-band high-resolution spectrum, the He I 1.700 μm line is redshifted ($\sim$300 km s^{-1}). This feature is strong in the spectra of P Cygni (Fig. 2*a*), southern hemisphere LBVs (McGregor et al. 1988b), and it has also been detected in the AF star (Fig. 4*c*; Najarro et al. 1993).

3.5. *IRS 1W*

3.5.1. *Low-Resolution Spectra*

We find Brγ and weak He I 2.058 μm line emission superposed on strong continuum emission throughout the IRS 1W region. The strength of the Brγ line emission reaches a maximum 5" east and 5" south of IRS 7. No appreciable 2.058 μm line emission was discovered south or east of the Brγ maximum, but the He I line did appear more convincingly 1" and 2" to the north. This contradicts the results of Krabbe et al. (1991) who find a compact He I 2.058 μm source 1".3 east and 0".4 south of the location of the Brγ maximum. In 1", 0.8% resolution imaging spectroscopy of the central parsec in the He I 2.058 μm line, Tamblyn et al. (1993, private communication) also find no evidence for a compact He I emission-line source at IRS 1W. Their data were obtained in 1993 May. The 2.058 μm line lies within a band of strong atmospheric absorption, making corrections for telluric absorption difficult. This fact may have contributed to an error by one of the authors. Alternatively, there may be actual variability in the He I emission (our data were obtained more than a year after the observations of Krabbe et al.). Tamura et al. (1993) have monitored the "He I stars" of Krabbe et al. on timescales as long as one year and found the K magnitude of IRS 1W to be constant to within 0.1 mag. However, their survey is not sensitive to the apparent level of variability in the He I 2.058 μm line, and IRS 1W was not monitored during the interval between our observations and those of Krabbe et al. The low-resolution composite spectrum extracted at the position of the Brγ maximum is presented in Figure 7*a*.

In the low-resolution H-band spectrum (extracted at the position of the Brγ maximum) there are weak features at 1.59, 1.64, 1.68, 1.72, and 1.76 μm, which may be emission lines or simply the result of poor sky subtraction.

3.5.2. 2.08–2.19 μm *High-Resolution Spectra*

The only clear line detection in the high-resolution, 2.08–2.19 μm spectrum of IRS 1W (Fig. 7*b*) is a marginally resolved Brγ line. We find the Brγ line to have a redshift of 110 km s^{-1} and a line width of 390 km s^{-1}, but we find no evidence for a maximum in the Brγ line width at IRS 1W.

3.5.3. 1.57–1.75 μm *High-Resolution Spectra*

There are strong lines in the 1.57–1.75 μm, high-resolution spectrum of IRS 1W (Fig. 7*c*) at 1.7359, 1.6819, and 1.6420 μm, which we identify as Br10, Br11, and Br12, respectively. The Br11 and Br12 lines have a greater redshift than the Br10 and Brγ lines, which could be due to contributions from Fe II $z\ ^4F_{9/2}$–$c\ ^4F_{9/2}$ (1.688 μm) and [Fe II] $a\ ^4F_{9/2}$–$a\ ^4D_{7/2}$ (1.644 μm), respectively. The line strengths (Table 6) of the Br11 and Br12 lines are also consistent with a blend of H I lines with the Fe II and [Fe II] lines. The strengths of both lines are greater than that of Br10, and are comparable to that of Brγ. Depoy (1992) has detected extended [Fe II] 1.644 μm emission in a 4".8 beam centered near IRS 1W.

There are also two broad unidentified features that are apparently blends of lines. One is centered at 1.709 μm, and the other at 1.598 μm. At least one component of each of these blends may be due to [Fe II]. There are [Fe II] lines at 1.598 μm ([Fe II] $a\ ^4F_{7/2}$–$a\ ^4D_{3/2}$) and at 1.710 μm ([Fe II] $a\ ^4F_{5/2}$–$a\ ^4D_{3/2}$). The 1.709 μm feature is most likely not associated with He I 1.700 μm line emission, because such an identification would suggest a prohibitively large redshift for either component.

The absence of He I 1.700 μm line emission is especially noteworthy, for none of the He I lines typically associated with strong He I 2.058 μm emission in emission-line stars (1.7002 μm and 2.112/3 μm) are evident in the high-resolution spectra of IRS 1W (Figs. 6*b* and 6*c*). This is consistent with the detection of weak, extended He I 2.058 μm emission in the low-resolution K-band spectrum obtained at the position of the IRS 1 Brγ peak.

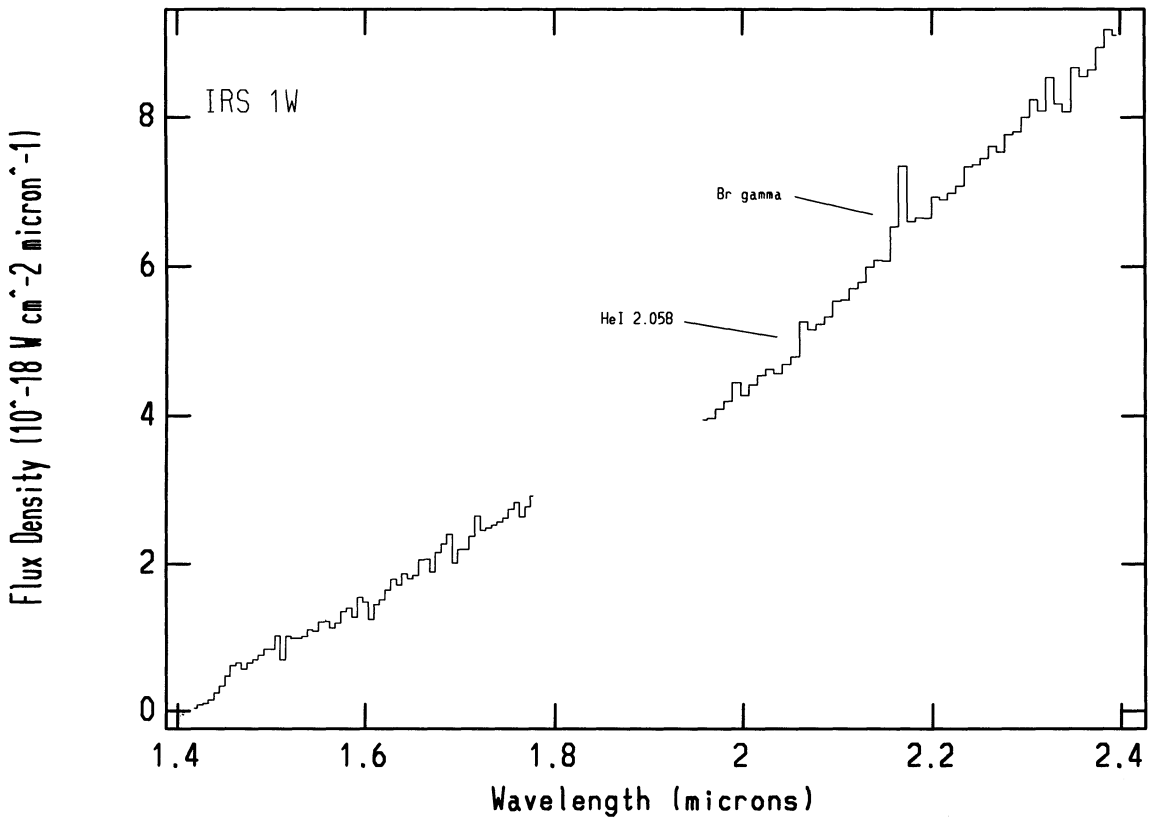

FIG. 7*a*

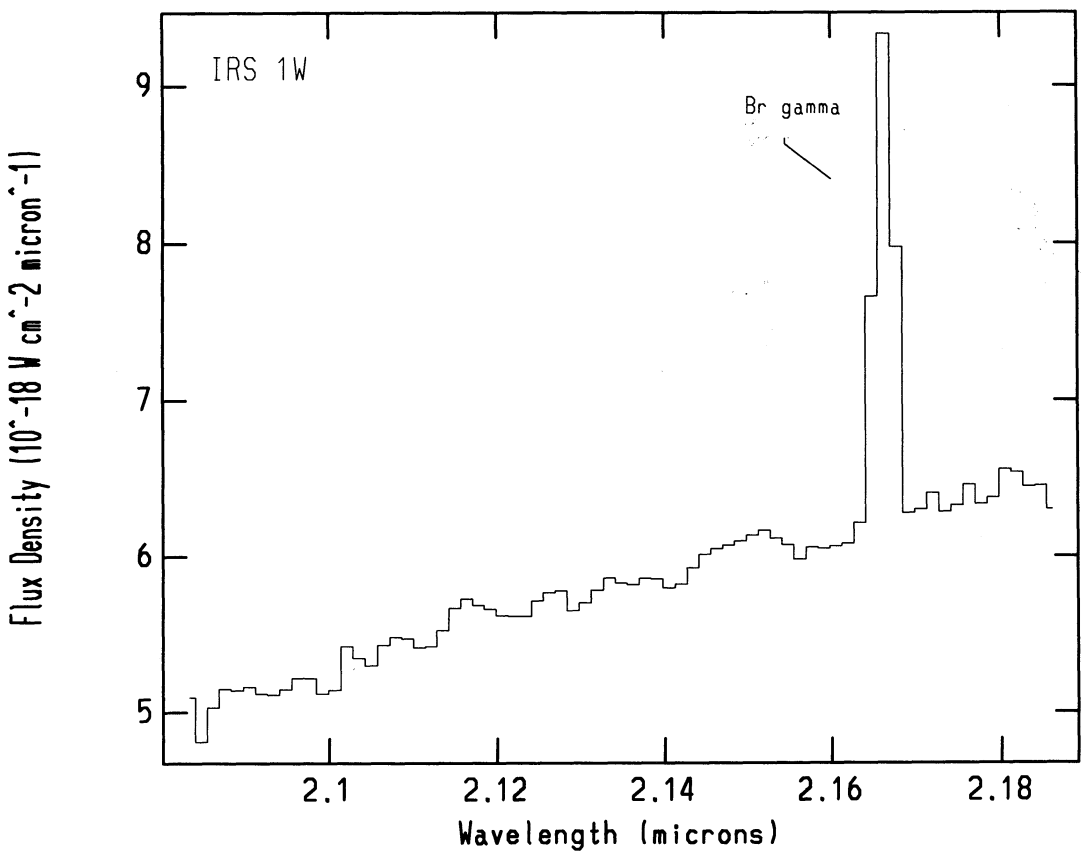

FIG. 7*b*

FIG. 7.—(*a*) *H*/*K* composite, low-resolution ($R \simeq 250$) spectrum of Galactic center source IRS 1W. (*b*) The 2.08–2.19 μm high-resolution ($R \simeq 850$) spectrum of Galactic center source IRS 1W. (*c*) The 1.57–1.75 μm high-resolution ($R \simeq 800$) spectrum of Galactic center source IRS 1W.

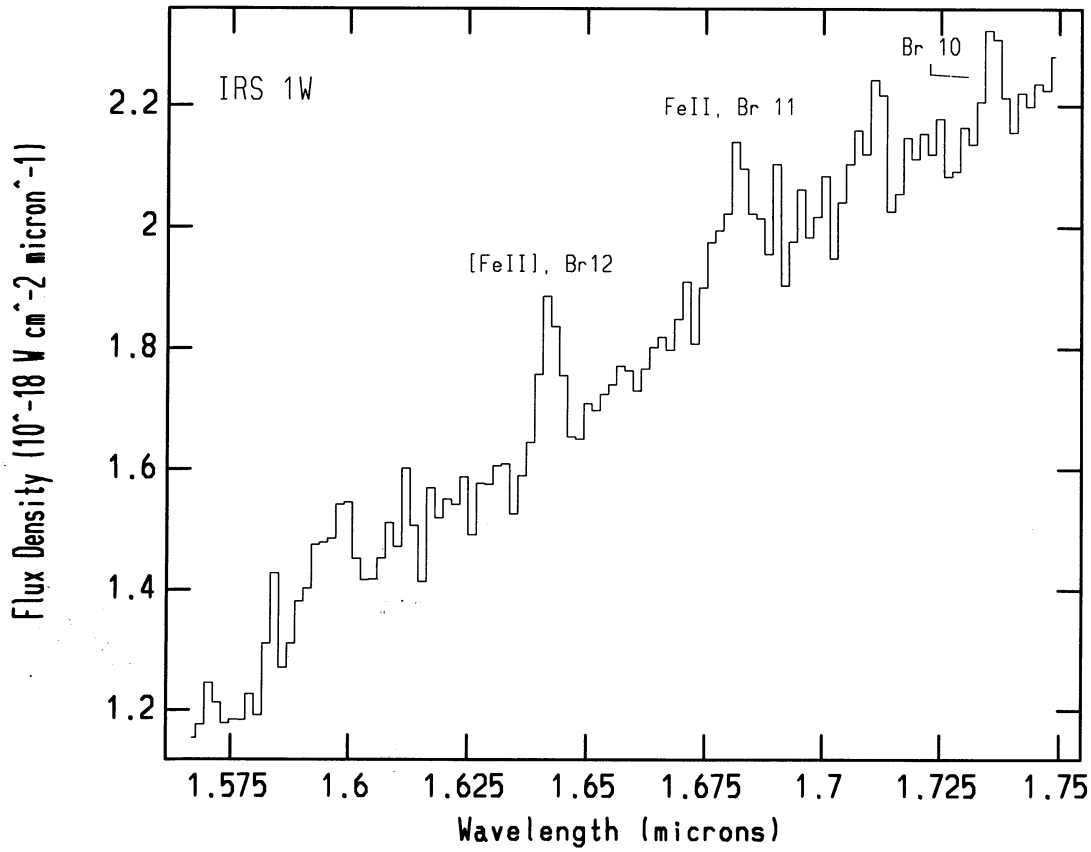

FIG. 7c

3.6. *IRS 16*

Spectra from four compact components of IRS 16 (16NE, 16NW, 16C, and 16SW) were extracted from our long-slit spectra and are presented in Figure 8. The relative offsets in right ascension for the IRS 16 source apertures were calculated from the positions given in Tollestrup et al. (1989). For IRS 16SW, the average of "16SW-E" and "16SW-W" was used. The locations of the source and background apertures for each IRS 16 source can be found in Table 1. Because of the crowded nature of the IRS 16 region, the IRS 16C aperture overlaps slightly with both the IRS 16NE and IRS 16NW apertures.

The low-resolution spectra of the four compact IRS 16 components are all dominated by Brγ and He I 2.058 μm lines with large F(He I 2.058 μm)/F(Brγ) line ratios. The line strengths can be found in Table 7. Longward of the Brγ line, several weak absorption features are evident at 2.29, 2.32, 2.35, and 2.37 μm, corresponding to the ^{12}CO (2–0), ^{12}CO (3–1), ^{13}CO (2–0), and ^{12}CO (4–2), and ^{13}CO (3–1) and ^{12}CO (5–3) band heads, respectively. These CO absorption features are characteristic of the unresolved concentration of late-type stars whose density peaks in the central parsec of the Galaxy (Allen 1987). Our background subtraction technique was unsuccessful in removing the entire contribution from the late-type population

TABLE 6

LINE IDENTIFICATIONS, FLUXES, AND EQUIVALENT WIDTHS FOR IRS 1W

Observed[a] Wavelength (μm)	Line Identification	Observed Flux[b] ($\times 10^{-22}$ W/cm^2)	Dereddened Flux[c] ($\times 10^{-20}$ W/cm^2)	Equivalent Width (Å)
1.6420 (4).....	[Fe II] $a\ ^4F_{9/2}$–$a\ ^4D_{7/2}$ (1.644 μm) H I 12–4 (1.6407 μm)	12.0	11.3	7
1.6819 (8).....	Fe II $z\ ^4F_{9/2}$–$c\ ^4F_{9/2}$ (1.688 μm) H I 11–4 (1.6806 μm)	23.6	12.2	9
1.7359 (5).....	H I 10–4 (1.7362 μm)	6.6	3.8	3
2.066[d].....	He I $2s\ ^1S$–$2p\ ^1P$ (2.058 μm)	32.0	7.3	6
2.1663 (3).....	H I 7–4 (2.1655 μm)	95.0	16.4	15

[a] The number in parentheses is the uncertainty in Å.

[b] ±20%.

[c] To obtain the dereddened fluxes, the entire spectrum was dereddened ($A_V = 27$, Wade et al. 1987) assuming a $\lambda^{-1.6}$ reddening law (Cardelli et al. 1989), and the fluxes were remeasured.

[d] The He I $2s\ ^1S$–$2p\ ^1P$ (2.058 μm) data are from the low-resolution spectrum.

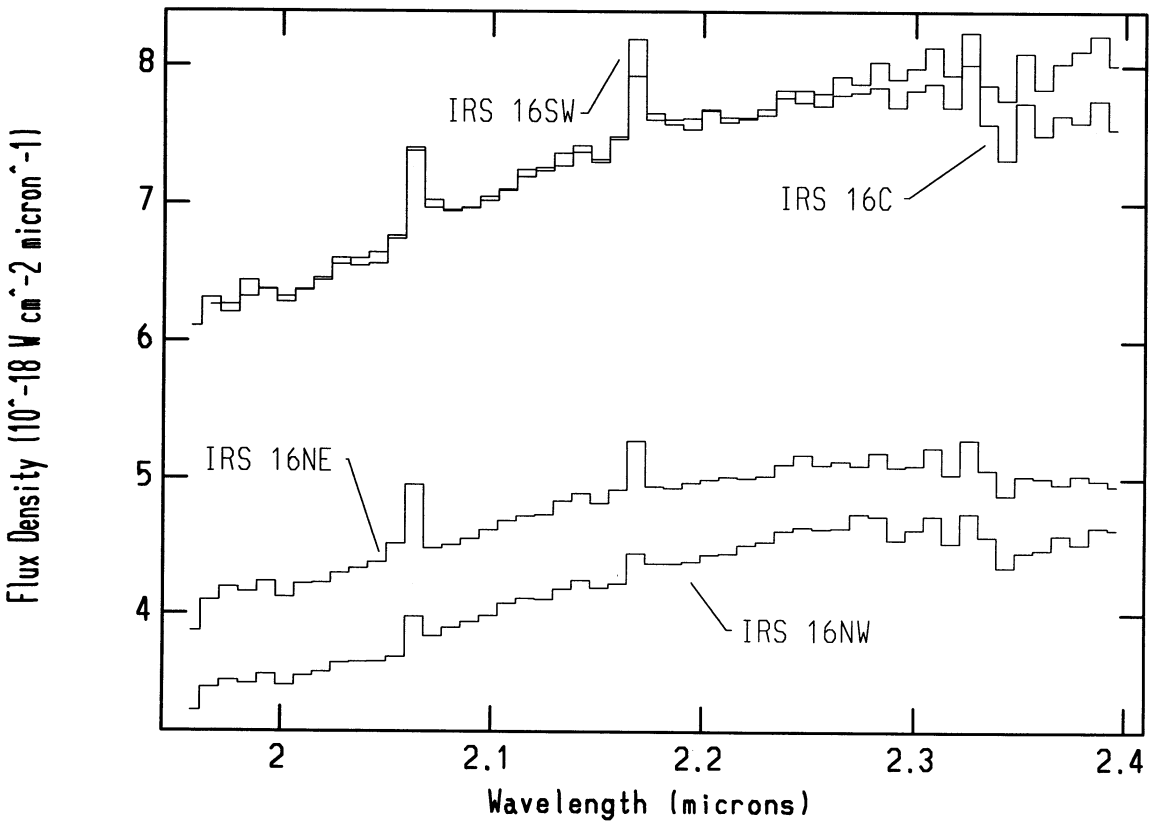

FIG. 8.—Low-resolution ($R \simeq 250$) K-band spectra of IRS 16NE, IRS 16NW, IRS 16C, and IRS 16SW

because for the IRS 16 sources, the background apertures were necessarily farther away from the source apertures than was the case for the other Galactic center sources.

The high-resolution K-band spectra provide little new information and are not presented. There is Brγ line emission in all four high-resolution K-band spectra, but there is, at most, marginal evidence for He I 2.112/3 μm emission in the spectra of IRS 16NW and 16C. The redshifts and line widths obtained from the Brγ line in each of the high-resolution K-band spectra are provided in Table 7 and discussed below.

The Brγ line is broadest at the position of IRS 16NW, where we measure a width of 590 km s^{-1}. The remaining sources have Brγ line widths in the 400–500 km s^{-1} range. For three of the four sources, the Brγ lines are also redshifted. At IRS 16NE and 16C we measure redshifts of 180 and 125 km s^{-1}. The Brγ line at IRS 16NW is shifted by 110 km s^{-1}, and at IRS 16SW by -40 km s^{-1}.

3.7. *IRS 34 and IRS 6E*

The low-resolution K-band spectra of IRS 34 and IRS 6E (Fig. 9) are also characterized by Brγ and He I 2.058 μm line emission with large F(He I 2.058 μm)/F(Brγ) ratios. The Brγ lines in the high-resolution spectra are broad (450–500 km s^{-1}) and blueshifted (Table 7). At IRS 6E, the Brγ line emission is

TABLE 7

PROPERTIES OF THE COMPACT STELLAR WIND SOURCES

Source	Brγ Flux[a] ($\times 10^{-20}$ W/cm^2)	Brγ Equivalent Width (Å)	v_0[b] (km s^{-1})	Δv_{FWHM}[b,c] (km s^{-1})	He I 2.058 μm Flux[a] ($\times 10^{-20}$ W/cm^2)	He I 2.058 μm Equivalent Width (Å)
P Cygni	1020	45	−15	440	1810	73
AF Source	14.4	82	180	890	28.2	110
IRS 13	12.5	28	−40	505	10.1	23
IRS 1W	16.4	15	110	390	7.3	6
IRS 16NE	8.2	9	180	480	13.3	13
IRS 16NW.....	3.5	6	110	590	3.4	4
IRS 16C.....	10.6	8	125	500	15.8	10
IRS 16SW	16.2	14	−40	410	17.0	13
IRS 34	4.0	10	−125	500	5.3	12
IRS 6E-N	6.8	24	−55	455	5.7	21

[a] Dereddened fluxes (±20%) using $A_V = 1.6$ for P Cygni, $A_V = 27$ for Galactic center sources, and a $\lambda^{-1.6}$ reddening law.
[b] From Brγ line in high-resolution spectra ($\sim \pm 50$ km s^{-1}).
[c] Measured width ($\sim \pm 60$ km s^{-1}), not deconvolved from instrumental profile (350 km s^{-1}).

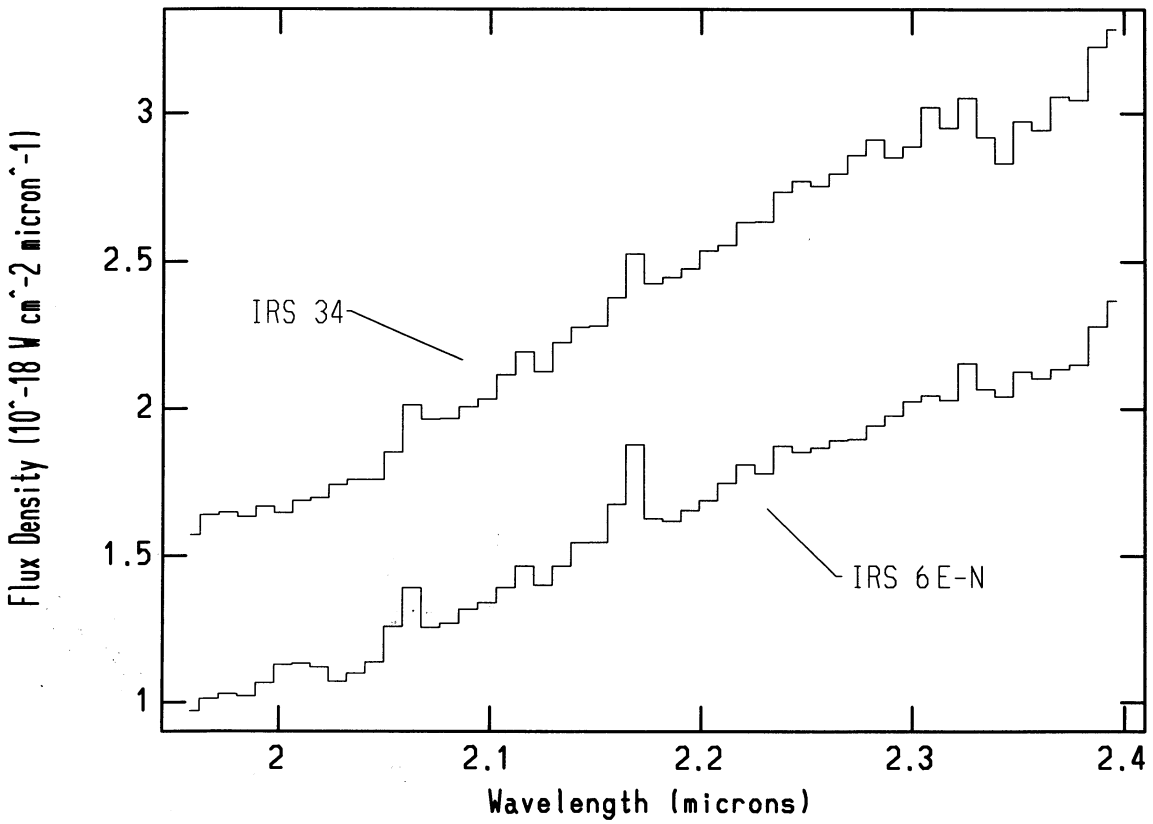

FIG. 9.—Low-resolution ($R \simeq 250$) K-band spectra of IRS 34 and IRS 6E-N

extended and reaches a maximum with our slit positioned 5″ south of IRS 7. However, the He I 2.058 μm line emission does not occur at the same slit position as the maximum of the Brγ line emission. We clearly detect He I 2.058 μm line emission with the slit positioned 4″ south of IRS 7, but find only marginal He I 2.058 μm line emission at the 5″ south slit position. The position of the He I line emission is coincident with a shoulder of K-band emission that extends northeast from IRS 6E on the occultation map of Simon et al. (1990). This position also agrees with the coordinates of a "He I star" discovered by Krabbe et al. at IRS 6. We will call the He I emission-line source IRS 6E-N.

3.8. *Multiplicity of the AF Source, IRS 6E, IRS 13, and IRS 1W*

We find two distinct *spectral* components to the AF source by extracting apertures from slightly different positions in our long-slit spectra. For both the low- and high-resolution AF source data, the spectra were extracted from data obtained with the slit nominally positioned 13″ south of IRS 7 (Fig. 3). The AF spectrum can also be extracted from data taken at the 12″ south position. When the 12″ south data were examined, it was found that the continuum emission in the vicinity of the AF source reaches a maximum ~0.″8–2.″4 farther west of IRS 12N than does the line emission. The spectrum extracted at the position of the line emission maximum (~3.″5 west of IRS 12N) resembles that of the AF source in Figure 4*b* but with weaker line strengths, indicating that the beam was not centered on the line emitting region in the 12″ south data. A spectrum extracted ~5.″2 west of IRS 12N, however, shows no emission lines (Fig. 10) and is consistent with a stellar continuum spectrum, such as that of the B0V star, τ Sco. After comparison of the spatial profile of the 12″ south data with our unpublished, 1″ resolution, K-band image, we believe that the "AF continuum source" (AF_{cont}) corresponds to a faint unnamed source which lies 2.″4 W and 1.″0 N of the "AF emission-line source" (AF) and which is also visible in the K-band image of Depoy & Sharp (1991).

In 2.2 μm observations of lunar occultations of the Galactic center, Simon et al. (1990), resolve both IRS 13 and IRS 1W into pairs of stars. The components of IRS 13 are separated by approximately 1.″2 east-west and have K magnitudes of 9.4 and 10.3. The components of IRS 1W are separated by 0.″4 east-west and have K magnitudes of 9.2 and 9.7. In recent 0.″15 resolution K-band images of the Galactic center, Eckart et al. (1993) also resolve IRS 13 and IRS 1W into more than one component each. By extracting apertures from slightly different positions in our long-slit, K-band, high-resolution spectra, we attempted to isolate distinct spectral components in these sources. Spectra from different offset positions south of IRS 7 were also examined. For IRS 13 and IRS 1W, only one spectral component was detected. Since the magnitudes of the two components in both IRS 13 and IRS 1W are comparable, the fact that only one emission-line spectrum was detected could imply that both components are emission-line stars. Recall that for IRS 6E we found a He I emission-line source to the north (IRS 6E-N) and a Brγ source to the south.

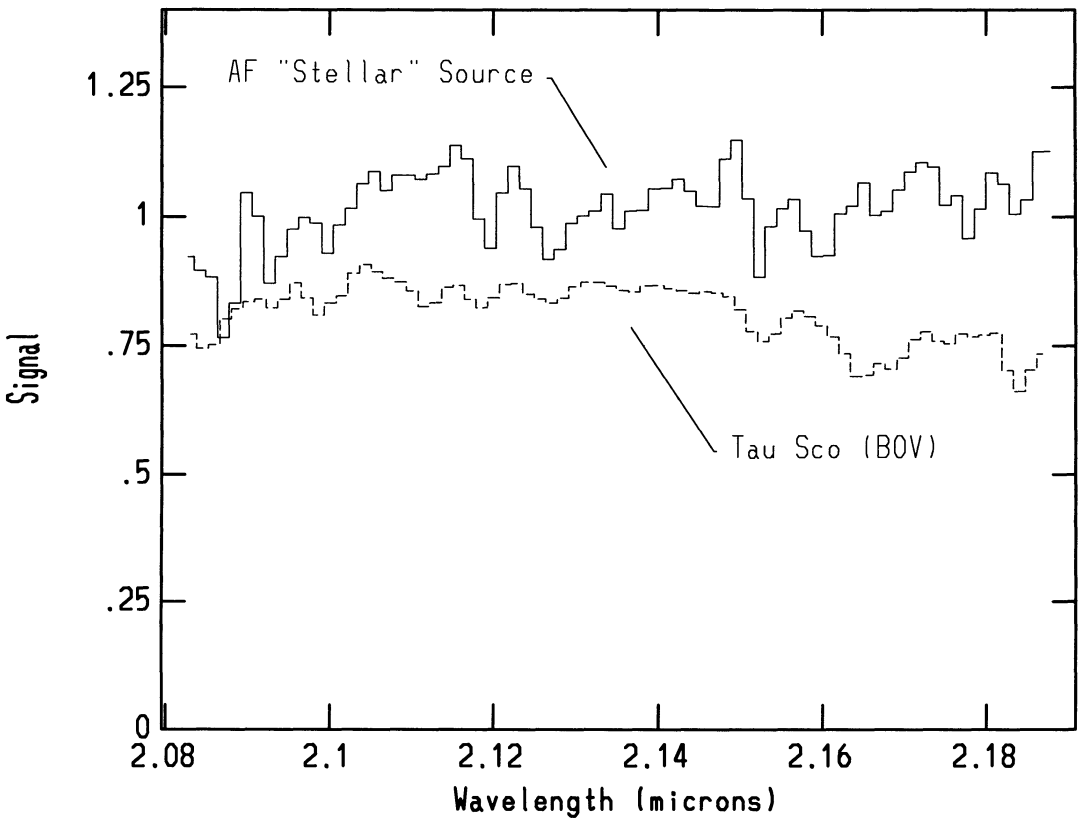

FIG. 10.—A 2.08–2.19 μm high-resolution ($R \simeq 850$) spectrum extracted 5".2 west IRS 12N with the slit nominally positioned 12" south of IRS 7. This shows the "AF continuum source" (AF_{cont}). For reference, the spectrum of a B0V star (Tau Sco) has also been plotted. The intensity scale is arbitrary. Both stars were normalized by their mean signal. Tau Sco was then shifted down by 0.2 units.

4. DISCUSSION

4.1. *He/H Ratios*

The line ratios, F(He I 2.058 μm)/F(Brγ) > 0.60, F(He I 1.700 μm)/F(Brγ) > 0.13, and F(He I 2.112/3 μm)/F(Brγ) > 0.03 are typically interpreted to indicate an overabundance of helium (Krabbe et al. 1991; Allen et al. 1985; and McGregor et al. 1988a). Several caveats are in order, however. The F(He I 2.058 μm)/F(Brγ) ratio is dependent upon the relative volumes of He^+ and H^+, the relative ionization fractions in the He^+ zone, as well as the velocity gradient in the emission region (Shields 1993; Najarro et al. 1993; Simon et al. 1983). Furthermore, all of the above ratios were calculated assuming case B recombination, but case B is inappropriate for emission-line stars. Recently, Najarro et al. (1993) have developed a more complicated wind model which they have applied to the AF source line ratios and widths. The new model indicates that the AF source has an enhanced He abundance ($N_{He}/N_H \sim 1$–1.67). Thus, we also suspect an enhanced He abundance in the other sources which have large He I/Brγ line flux ratios, including P Cygni, IRS 13, IRS 16NE, IRS 16NW, IRS 16C, IRS 16SW, IRS 34, and IRS 6E-N (Table 8). IRS 1W has a small F(He I

TABLE 8

He I TO Brγ LINE FLUX RATIOS[a]

Source	He I 1.700 μm/Brγ[b]	He I 2.112/3 μm/Brγ[b]	He I 2.058 μm/Brγ[b]
P Cygni	0.59	0.25	1.77
AF Source	0.61	0.41	1.96
IRS 13	0.38	0.36	0.81
IRS 1W	<0.18	<0.14	0.45
IRS 16NE	...	...	1.62
IRS 16NW.....	...	...	0.97
IRS 16C.....	...	...	1.49
IRS 16SW	...	...	1.05
IRS 34	...	...	1.33
IRS 6E-N	...	...	0.84

[a] Using dereddened line fluxes from Tables 2–7.
[b] ±28%.

2.058 μm)/F(Brγ) ratio, and such an analysis cannot be performed for the WN6 star because the Brackett lines cannot be isolated.

4.2. *Brackett Line Ratios*

As is found in known early-type emission-line stars, the Brγ/Br10, Brγ/Br11, and Brγ/Br12 line ratios are smaller than expected from case B recombination for P Cygni, the AF source, and IRS 13. Models of line formation in mass-loss winds predict small ratios of Brγ line flux to that of higher order Brackett lines, but the wind models alone cannot explain the higher order Brackett line flux ratios we obtain. Following the procedure outlined by Simon et al. (1981, 1983), and assuming a constant velocity ($v_{\rm flow} \sim 100$ km s^{-1}) mass-loss wind with a mass-loss rate of $10^{-6}\,M_\odot$ yr^{-1} and a temperature of 10^4 K, we calculate that for the AF source, the dereddened Br11/Br12 and Br10/Br11 ratios are consistent with a [Fe II] 1.644 μm contribution to Br12 as high as 40% and a N IV 1.736 μm contribution to Br10 as high as 25%. Note that a similar conclusion is reached if case B recombination (Osterbrock 1989) is assumed because although the Brα and Brγ lines are optically thick in the wind model (Simon et al. 1983), the Br11/Br12 and Br10/Br11 line ratios remain relatively unaffected. For IRS 13, the Br10/Br11 and Br10/Br12 line flux ratios yield an Fe II 1.688 μm contribution to Br11 of 20%, and an [Fe II] 1.644 μm contribution to Br12 of 25%. The strengths of the Br10 and Br11 lines in P Cygni suggest that there are significant contributions from the N IV 1.736 μm and Fe II 1.688 μm lines, respectively.

In the spectrum of IRS 1W, the dereddened Br10 to Brγ line flux ratio is consistent with case B recombination, indicating that the Brackett lines may not be formed in a mass-loss wind. The Br10/Br11 and Br10/Br12 line ratios imply that $\sim$75% of the Br11 line flux is due to Fe II 1.688 μm line emission, and that $\sim$80% of the Br12 line flux is due to [Fe II] 1.644 μm. A Brackett line ratio analysis cannot be made for IRS 6E-N, IRS 34, and the IRS 16 sources because the Br10, Br11, and Br12 lines were not detected.

4.3. *Identification of the Galactic Center Sources*

4.3.1. *The AF Source and IRS 13*

As in many LBVs and WN9/Ofpe stars, IRS 13 and the emission-line component of the AF source both appear to be sources of Fe line emission. For IRS 13 we are uncertain whether the Fe contributions are intrinsic to a wind source, or due to extended emission in the "bar." Depoy (1992) has found [Fe II] 1.644 μm emission in the vicinity of IRS 13 with a similar spatial distribution as that of the Brγ emission at 4.″8 spatial resolution. There is also extended [Fe III] emission throughout the central parsec of the Galaxy which peaks within 0.″5 of the maximum of the Brγ line emission at IRS 13 in 1″ spatial resolution, Fabry-Perot observations (Lutz et al. 1993). Recall that we detect a weak [Fe III] line (2.145 μm) in our IRS 13 spectrum. Lutz et al. claim that this [Fe III] emission peak is due to limb brightening at the edge of an expanding bubble. However, the coincidence of the Brγ and [Fe III] emission peaks, and the pointlike nature of the [Fe III] contours suggests an explanation where IRS 13 is, itself, a source of [Fe III] emission. The redshifts of the Brγ and [Fe III] lines in our spectra differ by less than 1 σ and do not rule out this explanation. Fe III features have been observed in the visible spectrum of R127, a WN9/Ofpe star which suddenly acquired the spectral characteristics of an LBV at photometric maximum (Stahl et al. 1983).

Both the AF source and IRS 13 spectra exhibit anomalous He I to Brγ line ratios which indicate an enhanced He abundance (see § 4.1). A large ratio of Brα line flux to radio continuum emission in the AF source, and broad emission lines in both sources have led many authors to assert that the emission lines are formed in mass-loss winds. Our measured Brackett line ratios confirm this hypothesis. As a result of these Brackett line ratios and widths, the enhanced He abundances, and probable Fe line emission, we identify the dominant exciting source(s) of IRS 13, and the emission-line component of the AF source as wind sources (LBV at minimum or WN9/Ofpe). Allen et al. (1990) suggest that the AF source is a WN9/Ofpe star based on its K-band spectrum, but identification of the AF source as an LBV at minimum is just as likely. It has been suggested that the two classifications are related, and the WN9/Ofpe classification may refer to the photometric minimum state of an LBV. Unambiguous identifications will require an observing program in which these sources are monitored for variability in their emission lines.

4.3.2. *IRS 1W*

The spectrum of IRS 1W is similar to spectra of LBVs at photometric maximum (see Appendix) such as S Dor, but there are also spectral characteristics which imply that IRS 1W is not a wind source. First, the dereddened Br10 to Brγ line flux ratio in IRS 1W is consistent with case B recombination. Furthermore, the broad lines in the IRS 1W region may be the result of mass motion in the "northern arm" rather than stellar winds at IRS 1W. Our Brγ line width is comparable to the instrumental profile of $\sim$350 km s^{-1}, but Herbst et al. (1993b) find that the line widths in their data do not peak at the IRS 1W position as they might were IRS 1W a wind source. The Brγ line width at IRS 1W is greater than that found for the diffuse Brγ emission in the "northern arm" northeast of IRS 1W, but slightly less than that found to the southwest. Finally, the Fe line emission we detect in our long-slit spectra appears extended rather than peaked at IRS 1W.

In contrast to the findings of Krabbe et al. (1991), we find no evidence for a compact He I emission-line source at IRS 1W. We also do not detect He I 2.112/3 or He I 1.700 μm emission, two features that are often associated with strong He I 2.058 μm emission in the spectra of LBVs and WN9/Ofpe stars. Our data were obtained more than a year after that of Krabbe et al., so it is possible that a compact He I emission line source at IRS 1W is variable. LBVs are known to have variable line emission on short timescales. HR Carina, for instance, showed a decrease of a factor of 3 in its He I 2.058 μm emission in less than two years (McGregor et al. 1988a). Other LBVs and WN9/Ofpe stars have shown similar radical changes in their spectra over short periods of time (see Appendix). Thus it is possible that IRS 1W contains an LBV in a quiescent state. Careful temporal monitoring of the spectrum of IRS 1W is necessary to verify such an identification.

4.3.3. *The IRS 16 Sources, IRS 34, and IRS 6E-N*

With the exception of the AF source, IRS 34, and the IRS 16 sources (IRS 16NE, IRS 16NW, IRS 16C, and IRS 16SW) have the largest F(He I 2.058 μm)/F(Brγ) ratios of any sources in the central parsec. However, some of the line emission we detect may not be intrinsic to the compact sources. IRS 16NE, IRS 16C, and IRS 16SW are embedded in a ridge of broad line

emission where the "northern arm" and "bar" intersect. Geballe et al. (1991) find strong He I line emission throughout this region. Thus, at our spatial resolution, it is difficult to differentiate between the line emission from the ridge, and that of the compact sources. IRS 16NW and IRS 34 are more isolated, but their apertures still contain some extended emission. In 1″, 0.8% resolution imaging spectroscopy of the central parsec in the He I 2.058 μm line, Tamblyn et al. (1993) find that IRS 16NE, IRS 16C, and IRS 16NW are all compact He I emission-line sources. Note that IRS 16NW was not identified as a "He I star" by Krabbe et al. (1991). IRS 34 was not observed by Tamblyn et al., but since we detect He I 2.058 μm line emission at IRS 34 with the slit positioned 4″ south of IRS 7, but not at adjacent slit positions, we believe that IRS 34 is a compact He I emission-line source.

The F(He I 2.058 μm)/F(Brγ) ratio in IRS 6E-N is smaller than that of the IRS 16 sources, but the proximity of the He I source to the IRS 6E H II region suggests that some of the Brγ line emission in the IRS 6E-N spectrum may be extended emission from the H II region. The Brγ line emission reaches a maximum south of IRS 6E-N, and the Brγ line width and blueshift are much the same as that found throughout the extended IRS 6E H II region.

Our line widths and the fact that compact Brα sources without 5 and 15 GHz radio continuum counterparts have been discovered at IRS 16NE, IRS 16C, IRS 16NW, IRS 34, and IRS 6E argues for mass-loss winds in these objects. These five sources also appear to be compact He I emission-line sources with enhanced He abundances. Thus it is likely that these objects are early-type, emission-line stars. For IRS 16SW, such an identification is less compelling. Because we were unable to detect other He I (1.700 μm, 2.112/3 μm) and Brackett lines, or any Fe II lines ([Fe II] 1.644 μm, Fe II 1.688 μm, or Fe II 2.09 μm) in the IRS 16 spectra, less ambiguous classifications cannot be made. We can only exclude classical Be stars which do not have strong He I 2.058 μm line emission.

4.4. *WR Stars*

Unlike the comparison WR spectrum (HD 192163), none of the Galactic center sources show any evidence of He II line emission. Since He II lines are strong in the spectra of both WN and WC stars, we conclude that none of the Galactic center objects are WR stars. This is interesting because the WR phase is expected (Humphreys 1991; Maeder 1989) to last 50–100 times longer than the LBV phase ($\tau_{LBV} \sim 10^4$–10^5 yr), thus if massive star formation were proceeding continuously in the Galactic center, we would expect to observe 50–100 times more WR stars than LBVs. Since no WR stars are observed, we conclude that the massive stars in the Galactic center were created in a starburst $\sim 10^6$–10^7 years ago, and the older or more massive members of this population have just reached the LBV and WN9/Ofpe stages of post–main-sequence evolution. We have proposed more sensitive WR line emission searches.

4.5. *The Luminosity of the Central Parsec*

We have presented evidence (summarized in Table 9) that supports the existence of a cluster of compact stellar wind sources at the Galactic center. We use a simple model to estimate the luminosity of the Galactic center wind sources in order to determine if they can account for the total luminosity observed in the central parsec ($\sim 10^7\ L_\odot$). The dereddened 2.2 μm flux density of each source is ascribed to blackbody radiation at an assumed T_{eff} in order to deduce the stellar radius. The Stefan-Boltzmann law then gives the blackbody luminosity. This model should yield a reliable order of magnitude estimate for the luminosity of the Galactic center wind sources since it turns out to be a reasonable approximation for known LBVs and WN9/Ofpe stars. For example, P Cygni at a distance of 1.8 kpc has a temperature of 19,300 K and a 2.2 μm flux density of 1.5×10^{-15} W cm^{-2} μm^{-1}. The blackbody estimate yields a luminosity of $6 \times 10^5\ L_\odot$ which corresponds well with its measured bolometric luminosity of $7 \times 10^5\ L_\odot$ (Humphreys 1989). For other emission-line stars (McGregor et al. 1988a, b) the argument is frequently not as good, but the blackbody approximation does generally agree to within an order of magnitude.

Assuming $D_{GC} = 8$ kpc, and $T_{eff} \sim 20{,}000$ K (an average value for the types of emission-line stars we have considered which range from 15,000 to 30,000 K in effective temperature), the blackbody luminosities for the nine Galactic center sources range between 2×10^5 and $1 \times 10^6\ L_\odot$. This range of luminosities is typical of the values for emission-line stars given by McGregor et al. (1988a, b). As a cluster, the nine wind sources

TABLE 9

SUMMARY OF RESULTS FOR GALACTIC CENTER SOURCES

Source	Unusual[a] Brα Source	Compact He I Source	Anomalous He I/H Line Ratios	Brackett[b] Line Ratios	Identification	Comments
AF Source	Yes	Yes	Yes	Wind model	LBV or WN9/Ofpe	
IRS 13	No	Yes	Marginal[c]	Wind model	LBV or WN9/Ofpe	
IRS 1W	No	No	No	Case B	?	Variable He I line emission?
IRS 16NE	Yes	Yes	Yes	...	Emission-line star	
IRS 16NW.....	Yes	Yes	Yes	...	Emission-line star	
IRS 16C.....	Yes	Yes	Yes	...	Emission-line star	
IRS 16SW	No	No	Yes	...	?	
IRS 34	Yes	Yes	Yes	...	Emission-line star	
IRS 6E-N	Yes	Yes	Marginal	...	Emission-line star	

[a] Found to be a compact Brα source with a weak radio continuum counterpart, suggesting line formation in dense ionized winds (Forrest et al. 1987).

[b] The Brγ, Br10, Br11, and Br12 line flux ratios for emission-line stars are more consistent with models of line formation in mass-loss winds than Case B recombination (§ 4.2).

[c] For IRS 13 the He I 2.058 μm/Brγ ratio is marginal, but the He I 1.700 μm/Brγ and He I 2.112/3 μm/Brγ ratios are anomalous (§ 4.1).

contribute $\sim 5 \times 10^6 L_\odot$ to the luminosity of the central parsec (using the above estimation technique). This is already an appreciable fraction of the total luminosity. The fraction will increase as more early-type, emission-line stars are confirmed.

The effective temperatures of LBVs and WN9/Ofpe stars are typically less than 30,000 K (see Appendix), but far-infrared fine-structure line ratios constrain the effective temperatures of the exciting stars of H II regions in the Galactic center to be 32,000–35,000 K (Watson, Storey, & Townes 1980). This implies that a population of late O stars is responsible for supplying the ionizing flux. Assuming an electron temperature of 5000 K, the Galactic center radio continuum emission (Ekers et al. 1983) requires ~ 100 ionizing O9 and O9.5 stars which would then contribute $\sim 3 \times 10^6 L_\odot$ to the luminosity of the central parsec. Thus, the late O stars may supply the ionizing photons, but the emission-line stars contribute more than half of the total luminosity. This scenario is consistent with the starburst model discussed above.

We would like to thank Dick Joyce and the rest of the NOAO staff for their help with the CRSP observations and the subsequent data reduction. We would also like to thank Jim Houck at Cornell University who offered telescope time and helped us obtain the high-resolution, *H*-band observations of the Galactic center. We are grateful to Peter Tamblyn, George Rieke, Laird Close, Don McCarthy, and Marcia Rieke for providing us with results from their unpublished Galactic center data. Finally, we thank the referee, Mike Simon, for his detailed comments and suggestions.

This work has been supported by the Astronomical Society of New York, NASA, the National Science Foundation, and the National Geographic Society.

APPENDIX

EARLY-TYPE, EMISSION-LINE STARS

At the end of the main-sequence lifetimes, the most massive stars experience a phase of heavy mass loss, passing through a subset of the Of, LBV (luminous blue variable), WN9/Ofpe, and WR (Wolf-Rayet) phases on their way to becoming supernovae. Models show that stars initially more massive than 120 $M_\odot$ pass directly from the Of to the WR phase. Stars with an initial mass between 40 and 120 $M_\odot$ evolve to an LBV before becoming a WR star (Maeder 1989). These objects have emission-line spectra with broad line widths. Often the emission lines show "P Cygni" profiles. Models of line formation in mass-loss winds (Simon et al. 1983; Smith et al. 1987) explain the emission-line flux ratios, as well as the ratios of IR emission line flux to radio continuum flux density.

The LBV phase is characterized by photometric variability, a large intrinsic luminosity ($L \simeq 10^5$–$10^6 L_\odot$), and high mass-loss rates ($\geq 10^{-6} M_\odot$ yr^{-1}). Small photometric variations of less than a magnitude in the visible have been observed to occur at intervals from months to years. Moderate photometric variations of 1–2 visible magnitudes occur with periods on the order of tens of years, with stars going from the minimum to maximum state within a few months. The bolometric magnitude remains relatively constant during these moderate variations in visible magnitude. In addition to the moderate variations, sporadic violent ejections of large amounts of mass occur at intervals from hundreds to thousands of years which can correspond to photometric variations of greater than three visible magnitudes (Humphreys 1989). Of course, LBVs can also remain relatively quiescent for long periods of time. For example, P Cygni has remains relatively quiescent during this century (Bohannan 1989). Effective temperatures range from about 8000 K at photometric maximum to 16,000–30,000 K at minimum.

The spectra of LBVs are dominated by emission lines of H, He I, Fe II, and [Fe II]. At photometric maximum, the spectra of LBVs resemble those of cool A-type supergiants with weak H, He I, Fe II, and [Fe II] emission lines (Humphreys 1989). At infrared wavelengths, the He I lines may disappear altogether. The prototypical A-type LBV, S Doradus, has only Brγ and Fe II 2.09 μm emission lines in its 2.0–2.4 μm spectrum (McGregor et al. 1988a). At photometric minimum LBVs have B-type spectra with stronger emission lines. He I/H line flux ratios suggest an overabundance of He I. The spectra resemble those of a class of WR star precursors known as WN9/Ofpe stars (objects which are observed to have characteristics of both WN9 and Of stars in their visible spectra). It has been suggested that the LBV and WN9/Ofpe classifications are related (Walborn 1989; Bohannan 1990), and may be two states of a single class of object. There is documented evidence of a WN9/Ofpe star (R 127) acquiring the spectral characteristics of an LBV at maximum, and WN9/Ofpe characteristics have been observed to suddenly appear in the spectrum of the LBV, AG Carina, during a minimum phase (Walborn 1989; Bohannan 1990). Other WN9/Ofpe stars are known to be variable themselves (R84, R99, and HD 269582) (Humphreys 1989). Since WN9/Ofpe stars are considered to be WR star precursors, the relationship between LBVs and WN9/Ofpe stars supports the idea that LBVs are also the predecessors of WR stars (McGregor 1989; Humphreys 1989). The effective temperatures of WN9/Ofpe stars tend to lie at the upper end of the LBV temperature range ($\sim 30{,}000$ K), and they have similar luminosities.

LBVs are also spectrally similar to a class of objects known as Be or Be*p* stars. This spectral similarity, however, does not necessarily imply an evolutionary relationship. Be stars show lines of H I, Fe II, and [Fe II] in their NIR spectra, but have weak or nonexistent He I line emission. Be stars have weak He I line emission because they lack the large helium abundances of LBVs and WN9/Ofpe stars, whereas weak He I line emission in LBVs at photometric maximum is attributed to low effective temperatures. Be star temperatures are, in fact, comparable to those of LBVs at photometric minimum, but they are less luminous ($L \simeq 10^4$–$10^5 L_\odot$).

The WR class is also characterized by a large intrinsic luminosity ($L \geq 10^5 L_\odot$), heavy mass loss (10^{-5} to $10^{-4} M_\odot$ yr^{-1}), effective temperatures ranging from 30,000 to 90,000 K, and depleted hydrogen abundances (van der Hucht 1991). It is believed that the mass-loss winds are sufficient to strip away the outer atmosphere, exposing the stellar core and the by-products of hydrogen burning (Chiosi & Maeder 1986). The spectra of WR stars are thus dominated by emission lines of He II and nitrogen for stars of the WN subclass, and He II and carbon for those of the WC subclass. These emission lines can be as broad as several thousand km s^{-1}, about a factor of 10 larger than those in LBVs and a factor of 100 larger than those found in normal supergiant stars (van der Hucht 1991).

REFERENCES

Allen, D. A. 1987, in AIP Conf. Proc. 155, The Galactic Center, ed. D. C. Backer (New York: AIP), 1
Allen, D. A., Hyland, A. R., & Hillier, D. J. 1990, MNRAS, 244, 706
Allen, D. A., Jones, T. J., & Hyland, A. R. 1985, ApJ, 291, 280
Becklin, E. E., Gatley, I., & Werner, M. W. 1982, ApJ, 258, 135
Bohannan, B. 1989, in IAU Colloq. 113, The Physics of Luminous Blue Variables, ed. K. Davidson, A. F. J. Moffat, & H. J. G. L. M. Lamers (Dordrecht: Kluwer), 35
Bohannan, B. 1990, in The Properties of Hot Luminous Stars, ed. C. D. Garmany (San Francisco: ASP), 39
Bowen, I. S. 1947, PASP, 59, 196
Cardelli, J. A., Clayton, G. C., & Mathis, J. S. 1989, ApJ, 345, 245
Chiosi, C., & Maeder, A. 1986, ARA&A, 24, 329
Davidson, J. A., Werner, M. W., Wu, X., Lester, D. F., Harvey, P. M., Joy, M., & Morris, M. 1992, ApJ, 387, 189
Depoy, D. L. 1992, ApJ, 398, 512
Depoy, D. L., & Sharp, N. A. 1991, AJ, 101, 1324
Eckart, A., Genzel, R., Hofmann, R., Sams, B. J., & Tacconi-Garman, L. E. 1993, ApJ, 407, L77
Ekers, R. D., van Gorkom, J. H., Schwarz, U. J., & Goss, W. M. 1983, A&A, 122, 143
Felli, M., Stanga, R. Oliva, E., & Panagia, N. 1985, A&A, 151, 27
Forrest, W. J., Shure, M. A., Pipher, J. L., & Woodward, C. E. 1987, in AIP Conf. Proc. 155, The Galactic Center, ed. D. C. Backer (New York: AIP), 153
Geballe, T. R., Krisciunas, K., Bailey, J. A., & Wade, R. 1991, ApJ, 370, L73
Geballe, T. R., & Persson, S. E. 1987, ApJ, 312, 297
Gehrz, R. D., Hackwell, J. A., & Jones, T. W. 1974, ApJ, 191, 675
Genzel, R., & Townes, C. H. 1987, ARA&A, 25, 377
Herbst, T. M., Beckwith, S. V. W., Forrest, W. J., & Pipher, J. L. 1993b, AJ, 105, 956
Herbst, T. M., Beckwith, S. V. W., & Shure, M. 1993a, ApJ, submitted
Humphreys, R. M. 1989, in IAU Colloq. 113, The Physics of Luminous Blue Variables, ed. K. Davidson, A. F. J. Moffat, & H. J. G. L. M. Lamers (Dordrecht: Kluwer), 3
———. 1991, in IAU Symp 143, Wolf-Rayet Stars and Interrelations with Other Massive Stars in Galaxies, ed. K. A. van der Hucht & B. Hidayat (Dordrecht: Kluwer), 485
Krabbe, A., Genzel, R., Drapatz, S., & Rotaciuc, V. 1991, ApJ, 382, L19
Lacy, J. H., Achtermann, J. M., & Serabyn, E. 1991, ApJ, 380, L71
Lutz, D., Krabbe, A., & Genzel, R. 1993, ApJ, submitted
Maeder, A. 1989, IAU Colloq. 113, The Physics of Luminous Blue Variables, ed. K. Davidson, A. F. J. Moffat, & H. J. G. L. M. Lamers (Dordrecht: Kluwer), 15
McGregor, P. J. 1989, in IAU Colloq. 113, The Physics of Luminous Blue Variables, ed. K. Davidson, A. F. J. Moffat, & H. J. G. L. M. Lamers (Dordrecht: Kluwer), 165
McGregor, P. J., Hillier, D. J., & Hyland, A. R. 1988a, ApJ, 334, 639
McGregor, P. J., Hyland, A. R., & Hillier, D. J. 1988b, ApJ, 324, 1071
Najarro, F., Hillier, D. J., Kudritzki, R. P., Krabbe, A., Genzel, R., Lutz, D., Drapatz, S., & Geballe, T. R. 1993, A&A, submitted
Osterbrock, D. E. 1989, Astrophysics of Gaseous Nebulae and Active Galactic Nuclei (Mill Valley: University Science)
Rieke, G. H., & Lebofsky, M. J. 1982, in AIP Conf. Proc. 83, The Galactic Center, ed. G. R. Riegler & R. D. Blanford (New York: AIP), 194
———. 1985, ApJ, 288, 618
Rieke, G. H., Rieke, M. J., & Paul, A. E. 1989, ApJ, 336, 752
Sellgren, K., McGinn, M. T., Becklin, E. E., & Hall, D. N. B. 1990, ApJ, 359, 112
Shields, J. C. 1993, ApJ, 419, 181
Simon, M., & Cassar, L. 1984, ApJ, 283, 179
Simon, M., Chen, W. P., Forrest, W. J., Garnett, J. D., Longmore, A. J., Gauer, T., & Dixon, R. I. 1990, ApJ, 360, 95
Simon, M., Felli, M., Cassar, L., Fischer, J., & Massi, M. 1983, ApJ, 266, 623
Simon, M., Righini-Cohen, G., Fischer, J., & Cassar, L. 1981, ApJ, 251, 552
Smith, H. A., Fischer, J., Geballe, T. R., & Schwartz, P. R. 1987, ApJ, 316, 265
Stahl, O., Wolf, B., Klare, G., Cassatella, A., Krautter, J., Persi, P., & Ferrari-Toniolo, M. 1983, A&A, 127, 49
Tamblyn, P., Rieke, G. H., Close, L. M., McCarthy, D. W., & Rieke, M. J. 1993, private communication
Tamura, M., Werner, M. W., Becklin, E. E., & Phiney, E. S. 1993, ApJ, submitted
Tollestrup, E. V., Capps, R. W., & Becklin, E. E. 1989, AJ, 98, 204
Treffers, R. R., Fink, U., Larson, H. P., & Gautier, T. N., III. 1976, ApJ, 209, 793
Turner, D. G. 1985, A&A, 144, 241
van der Hucht, K. A. 1991, in IAU Symp. 143, Wolf-Rayet Stars and Interrelations with Other Massive Stars in Galaxies, ed. K. A. van der Hucht & B. Hidayat (Dordrecht: Kluwer), 19
Wade, R., Geballe, T. R., Krisciunas, K., Gatley, I., & Bird, M. C. 1987, ApJ, 320, 570
Walborn, N. R. 1989, in IAU Colloq. 113, The Physics of Luminous Blue Variables, ed. K. Davidson, A. F. J Moffat, & H. J. G. L. M. Lamers (Dordrecht: Kluwer), 27
Watson, D. M., Storey, J. W. V., & Townes, C. H. 1980, ApJ, 241, L46
Werner, M. W., Becklin, E. E., Stauffer, J., & Lee, T. 1991, BAAS, 23, 830
Werner, M. W., Tamura, M., Becklin, E. E., & Tokunaga, A. 1992, BAAS, 24, 1260
Yusef-Zadeh, F., Morris, M., & Ekers, R. D. 1989, in IAU Symp. 136, The Center of the Galaxy, ed. M. Morris (Dordrecht: Kluwer), 443

Note added in proof.—Further analysis of our CRSP data set has revealed two more early-type, emission-line stars in the central parsec of the Galaxy. One of them (IRS 9W) lies west of IRS 9 (within 3″), and the other is located 3″ north and 1″ west of the AF source. The latter source was identified as a "He I star" by Krabbe et al. (1991) and named AHH-NW (AF-NW in our nomenclature). We detect He I 2.058 μm, 2.112/3 μm, and Brγ line emission in our spectra of IRS 9W, and identify it as an LBV or WN9/Ofpe star. In our K-band spectrum of AF-NW, the He I 2.058 μm, 2.112/3 μm, and Brγ emission lines are clearly detected, and another feature that we identify as the He II (10–7) 2.189 μm line is detected at the 3–4 σ level. The relative line strengths coupled with our tentative detection of He II (10–7) 2.189 μm line emission in the AF-NW spectrum indicate that AF-NW is a WN7-8 star, making AF-NW the first "true" WR star detected at the Galactic center.